



Trends in hydrogel-based encapsulation technologies for advanced cell therapies applied to limb ischemia



Ana Letícia Rodrigues Costa^a, Stephanie M. Willerth^{b,c,d}, Lucimara Gaziola de la Torre^a, Sang Won Han^{e,*}

^a Department of Materials and Bioprocesses Engineering, School of Chemical Engineering, University of Campinas, Campinas, SP, Brazil

^b Department of Mechanical Engineering, University of Victoria, Victoria, BC, V8W 2Y2, Canada

^c Division of Medical Sciences, University of Victoria, Victoria, BC, V8W 2Y2, Canada

^d School of Biomedical Engineering, University of British Columbia, Vancouver, BC V6T 1Z4, Canada

^e Department of Biophysics, Escola Paulista de Medicina, Federal University of Sao Paulo, Sao Paulo, SP, Brazil

ARTICLE INFO

Keywords:

Limb ischemia
Electrostatic droplet extrusion
Micromolding
Microfluidics
3D bioprinting
Hydrogel

ABSTRACT

Ischemia occurs when blood flow is reduced or restricted, leading to a lack of oxygen and nutrient supply and removal of metabolites in a body part. Critical limb ischemia (CLI) is a severe clinical manifestation of peripheral arterial disease. Atherosclerosis serves as the main cause of CLI, which arises from the deposition of lipids in the artery wall, forming atheroma and causing inflammation. Although several therapies exist for the treatment of CLI, pharmacotherapy still has low efficacy, and vascular surgery often cannot be performed due to the pathophysiological heterogeneity of each patient. Gene and cell therapies have emerged as alternative treatments for the treatment of CLI by promoting angiogenesis. However, the delivery of autologous, heterologous or genetically modified cells into the ischemic tissue remains challenging, as these cells can die at the injection site and/or leak into other tissues. The encapsulation of these cells within hydrogels for local delivery is probably one of the promising options today. Hydrogels, three-dimensional (3D) cross-linked polymer networks, enable manipulation of physical and chemical properties to mimic the extracellular matrix. Thus, specific biostructures can be developed by adjusting prepolymer properties and encapsulation process variables, such as viscosity and flow rate of fluids, depending on the final biomedical application. Electrostatic droplet extrusion, micromolding, microfluidics, and 3D printing have been the most commonly used technologies for cell encapsulation due to their versatility in producing different hydrogel-based systems (e.g., microgels, fibers, vascularized architectures and perfusable single vessels) with great potential to treat ischemic diseases. This review discusses the cell encapsulation technologies associated with hydrogels which are currently used for advanced therapies applied to limb ischemia, describing their principles, advantages, disadvantages, potentials, and innovative therapeutic ideas.

1. Introduction

Blood vessels serve the fundamental role of ensuring that appropriate blood and oxygen supply is maintained throughout the whole body. However, the integrity of blood vessels can be affected by a combination of obesity, smoking, high blood pressure, hypercholesterolemia, diabetes, and genetics. The chance of these factors affecting our bodies increases with age and sedentariness [1].

Cardiovascular artery disease (CAD) and peripheral artery disease (PAD) are caused by obstruction of arteries, leading to decreased blood flow, which is known as ischemia. The leading cause of ischemia is

atherosclerosis. This condition arises when arteries become inflamed, which leads to the deposition of lipids in the artery wall, forming atheroma [2]. Ischemia occurs slowly and is usually asymptomatic at the beginning, making prevention and treatment difficult. Several effective drugs have been developed to control hypertension, dyslipidemia, and diabetes, which are the main risk factors for CAD and PAD, in addition to invasive surgical interventions [1]. However, these drugs and surgical interventions present several limitations due to the heterogeneity of the pathophysiological condition of each patient, which affects drug efficacy, side effects and surgery risk, especially for elderly and diabetic patients.

Therapy with cells or genetically modified cells (known as *ex vivo*

* Corresponding author.

E-mail address: sang.han@unifesp.br (S.W. Han).

<https://doi.org/10.1016/j.mtbio.2022.100221>

Received 26 November 2021; Received in revised form 28 January 2022; Accepted 12 February 2022

Available online 16 February 2022

2590-0064/© 2022 The Authors. Published by Elsevier Ltd. This is an open access article under the CC BY-NC-ND license (<http://creativecommons.org/licenses/by-nc-nd/4.0/>).

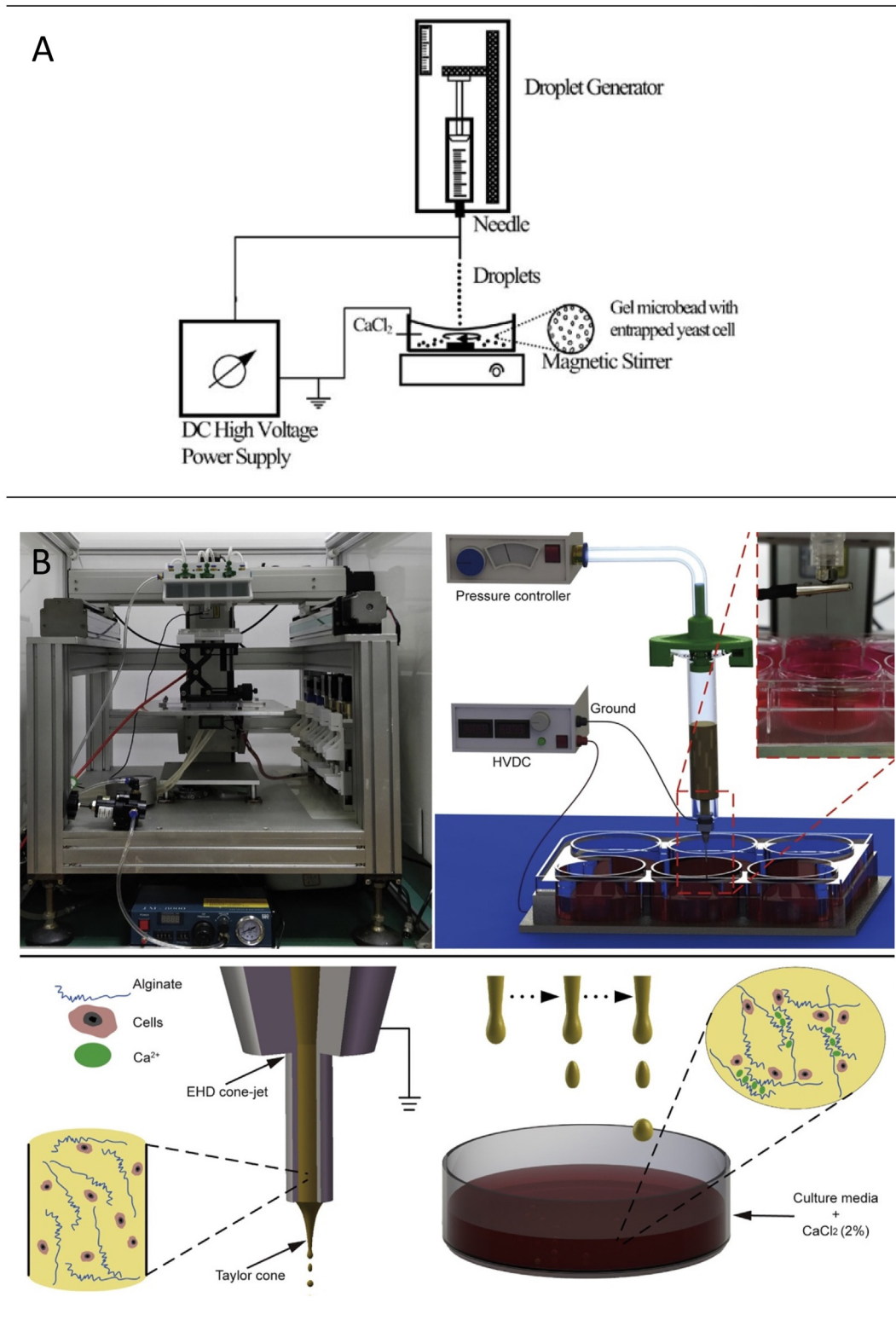


Fig. 1. A) Schematic experimental setup of the electrostatic droplet extrusion method [18]. B) Generation process of alginate microspheres with HEK293T cells, including experimental setup and droplet-dispensing system [29].

gene therapy) for limb ischemia is expected to result in high expression of growth factors that bind to their receptors on target cells, promoting angiogenesis [3]. The term “angiogenesis” is widely used to refer to the formation of new vessels. However, in biology, at least three pathways of vessel formation are designated in the adult phase: angiogenesis and vasculogenesis consist of the formation of new vessels from preexisting

vessels by sprouting and from a precursor of endothelial cells, respectively, and arteriogenesis consists of remodeling of collateral vessels to become more functional [4]. This review will use the term “angiogenesis” in general, *i.e.*, it refers to any of angiogenesis, arteriogenesis, and vasculogenesis, unless a specific form of vessel formation is mentioned.

Most cells secrete growth factors such as vascular endothelial growth

factor (VEGF), fibroblast growth factor (FGF), hepatocyte growth factor (HGF), and hypoxia-inducible factor-1 α (HIF-1 α) to stimulate cell proliferation and differentiation and other activities in autocrine and paracrine ways. Because the types of growth factors are related to the producing cells and their microenvironment, endothelial progenitor cells (EPCs), bone marrow-derived mononuclear cells (BM-MNCs), peripheral blood mononuclear cells (PB-MNCs), and mesenchymal stem cells (MSCs) have been mostly used for preclinical and clinical assays for the promotion of angiogenesis and immunomodulation to treat PAD [5]. Cells are generally injected directly into the skeletal muscle for therapy. However, challenges associated with a low transplantation rate are present due to cell leakage, and the loss of biological activity still needs to be overcome. In addition, leaks due to high initial concentrations of cells at the injection site can also cause contamination of other tissues, which is a concerning biosafety issue [6,7].

Hydrogel-based encapsulation technologies have emerged as promising approaches to overcome these challenges. Hydrogels, three-dimensional (3D) networks composed of crosslinked hydrophilic polymer chains, can be manipulated to resemble the extracellular environment of body cells and tissues, allowing their use in fields of regenerative medicine encompassing gene and cell therapies and tissue engineering [8]. Currently, hydrogels can be categorized into natural polymer-based hydrogels (e.g., alginate, gelatin, collagen, fibrinogen, and agarose) and synthetic polymer-based hydrogels (e.g., poly (lactic-co-glycolic acid), poly (ethylene glycol), and poly (ethylene glycol) diacrylate). Hydrogels obtained from natural polymers are more biocompatible and require mild gelling conditions; however, they exhibit low mechanical performance. Hydrogels for limb ischemia treatment require more than cell compatibility based on the mimetic extracellular matrix; they require defined mechanical and chemical properties based on the delivery route [9]. Thus, chemically modified biopolymers or hybrid hydrogels are promising materials to overcome this and other limitations of natural polymers, as they integrate the chemical, physical and biological advantages of each polymer, improving the performance of the cell immobilizing hydrogel. However, adjustments in the composition of biopolymers must also consider the degradation process of hydrogels since the cells must be able to replace the polymer matrix with their extracellular matrix to promote better *in vivo* integration over time. In general, cell encapsulation isolates live cells in polymeric matrices to protect against host antibodies and effector immune cells and allows bidirectional diffusion of low molecular weight molecules and bioactive compounds responsible for maintaining cell viability. Thus, advanced therapies based on the immobilization of cells in hydrogels aim at the release of molecules (e.g., growth factors) with therapeutic effects from confined cells or the release of these cells in the target tissue, promoting its repair and regeneration [10–12].

Different hydrogel-based systems, including microgels, fibers, vascularized architectures, and perfusable single vessels, have been produced from electrostatic droplet extrusion, micromolding, microfluidics, and 3D-printing technologies, aiming at the development of innovative therapies to treat ischemic diseases. To obtain full therapeutic activity from cells, encapsulation and delivery to the target organ require special attention to avoid the loss of cell integrity and biological activity. The cell metabolism and phenotype can be changed to adapt to a new microenvironment, causing loss of the expected therapeutic effect, and/or these cells can die via necrosis, triggering the inflammation process. Thus, systematic studies must be carried out to optimize the process parameters, minimize the adverse effects of the encapsulation processes on the cell biological response and improve the biostructure performance in terms of biocompatibility, physical properties, and biodegradation during angiogenic processes. Accordingly, this review points out the most current hydrogel-based encapsulation technologies for advanced cell therapies applied to limb ischemia. It also describes their principles, advantages, disadvantages, potentials, and future perspectives.

2. Encapsulation technologies for angiogenic therapy

2.1. Electrostatic droplet extrusion applied to ischemic diseases

Encapsulation of cells into hydrogel particles has been achieved using conventional methods, such as the air jet and dripping extrusion methods [13,14]. In this simple dripping extrusion process, the cells are initially suspended in a hydrogel precursor solution, which is dripped from a syringe into a bath containing the gelling agent. Finally, the cells are trapped in the three-dimensional network during gelation [11,13]. Although this method does not require any sophisticated instrumentation, controlling the resulting bead size and shape remains difficult, leading to the generation of macrogels (approximately 1500–5000 μm) with broad size distributions [13,15]. For biomedical applications, uniform smaller beads are better because they promote higher diffusion of nutrients and oxygen in the transplanted area and a greater probability of survival of immobilized cells [13]. These beads are known as microbeads and have diameters <200–1000 μm .

As an alternative, electrostatic extrusion is an advanced technology compared to simple extrusion methods [16,17]. It produces much smaller beads (diameter between 50 and 200 μm) with uniform size under mild stress conditions without using organic solvents and high temperatures. Electrostatic forces are used to break a liquid jet extruded through a needle tip connected to the high-voltage electrostatic generator (Fig. 1A) and, thus, to form a charged stream of small droplets [17,18]. Several factors can affect the diameter of droplets, such as the electrostatic potential, electrode distance, needle diameter, and polymer solution flow rate, as well as its properties, such as viscosity, density, and surface tension [16–19]. In addition, cells within the polymeric solution also change the flow dynamics of the electrostatic extrusion process due to electrostatic and physical interactions between the cells and polymer [18].

Some studies have already reported the production of injectable calcium alginate microbeads by electrostatic extrusion to deliver immobilized MSCs for tissue regeneration [20,21], and specifically for cell therapy applied to limb ischemia [22–26]. In general, although a high electric field is used in the droplet formation process, the applied electrical potential does not affect cell viability [17,18]. Moyer et al. [20] reported the production of viable adipose-derived stem cells (ADSCs)-laden microbeads <200 μm in size at a flow rate of 5 mL/h and an electrostatic potential of 7 kV. Moreover, ADSCs remained viable and showed signs of mitosis three months after percutaneous injection of these microbeads. Leslie et al. [21] also made injectable alginate microbeads smaller than 200 μm , which were persistent in implantation sites containing viable ADSCs. In this study, the controlled degradation of alginate was achieved by incorporating the enzyme lyase into alginate microbeads, since its nonenzymatic breakdown occurs very slowly in the human body.

MSCs secrete several soluble factors, with vascular endothelial growth factor (VEGF) being one of the most potent angiogenic factors in the treatment of ischemic diseases. Attia et al. [27] produced alginate-poly-L-lysine-alginate microcapsules (diameters ranging from 600 to 650 μm) loaded with *human bone marrow mesenchymal stem cells* (hBM-MSCs) via electrostatic extrusion. They showed increased VEGF production by hBM-MSCs 1 day postencapsulation, which was maintained for at least 4 weeks. Microencapsulation of cells in microbeads produced by electrostatic extrusion has opened new perspectives to treat ischemic diseases since this technique is easy to use under sterile conditions, reproducible and controllable. hBM-MSCs delivered from alginate microbeads produced by electrostatic extrusion were also used to treat ischemic tissue *in vivo*. Alginate microbeads supported the proangiogenic secretory activity of encapsulated hBM-MSCs, prevented cell incorporation into the host tissue, and significantly increased their therapeutic efficiency [22]. Furthermore, when outgrowth endothelial cells (ECs) and growth factors were combined in arginine-glycine-aspartic acid (RGD)-conjugated alginate injectable microbeads, the therapeutic potency to create new

blood vessels *in vivo* was increased compared to the use of a single material [25].

The ability of genetically modified cells (*ex vivo* gene therapy) to promote angiogenesis in a murine hindlimb ischemia model has also been explored [28,29]. Alginate microbeads produced by electrostatic extrusion containing HEK293T cells with stably integrated VEGF- α plasmids (Fig. 1B) were subcutaneously implanted into mice. The microspheres did not cause an inflammatory response, liver damage, or kidney damage in mice. On day 7, microbeads stably overexpressing VEGF promoted muscle regeneration and reduced apoptosis and toe necrosis. In addition, capillary densities and perfusion were increased in the mice that received these microbeads compared with those that received microbeads containing scramble-transfected HEK293T cells [29]. VEGF-secreting human umbilical vein endothelial cell (HUVEC)-microbeads were produced by electrospaying the methacrylate gelatin (GelMA) and alginate mixture followed by secondary crosslinking of GelMA with UV light and alginate hydrogel chelation using sodium citrate solution. VEGF-secreting HUVEC-GelMA microbeads induced the restoration of blood flow and neovascularization in a hindlimb ischemia mouse model. After 1 week, the blood flow increased from 20% to over 40%, and up to 60% recovery was reported after 4 weeks. In addition, only 10% of mice lost hindlimbs, while 30% maintained healthy limbs [28].

Microbeads produced by electrostatic extrusion were also used to visualize cell delivery and track cell distribution and engraftment through noninvasive imaging. hBM-MSCs encapsulated in alginate with barium sulfate or perfluorooctyl bromide showed high cell viability and high sensitivity for detection. hBM-MSC-encapsulated microbeads improved hindlimb perfusion in an endovascular rabbit model of peripheral artery disease with easy visualization of the therapeutic at the time of implantation and up to day 14 using clinical X-ray and/or magnetic resonance imaging systems. According to these studies, visible-cellular therapy permits physicians to confirm the accurate delivery and persistence of therapeutic payloads [23,26]. A comparison of cell-laden microstructures produced by electrostatic droplet generation is presented in Table S1 (supplementary material).

Currently, a good manufacturing practice (GMP)-encapsulator (BUCHI B-395 Pro encapsulator) has been commercialized to facilitate the encapsulation of cells in polymeric microbeads produced by electrostatic droplet extrusion [30]. The process is similar to the previously mentioned approach; however, it guarantees the sterile encapsulation of cells in a more efficient, reproducible, and controlled manner. Ludwinski et al. [24] used the GMP-encapsulator to generate SLG20 alginate microbeads encapsulated with murine bone marrow-derived macrophages. Intramuscular delivery of the encapsulated macrophages into the murine ischemic hindlimb resulted in increased cell retention compared with the injection of naked cells and an overall improvement in limb perfusion. In general, the electrostatic droplet extrusion technique represents a means of improving the effectiveness of cell-based therapies currently under investigation to treat limb ischemia.

2.2. Micromolding and microfluidics for therapeutic angiogenesis

2.2.1. Micromolding

Micromolding is a reproducible, versatile, and highly controlled method for manufacturing complex vascularized tissue architectures in hydrogel materials. In general, the manufacturing process includes the fabrication of the micromolds, casting of prepolymer solution on the micromolds, and removal of the solidified gel from the molds [31]. Thus, the materials used to produce micromolds should be sufficiently mechanically stable to maintain the pattern structure and allow easy removal of the solidified hydrogel. The micromolds can be made from a solid material (glass, silicone, poly (methyl methacrylate)) or a hydrogel, such as polyethylene glycol (PEG) [17,32,33]. However,

polydimethylsiloxane elastomer (PDMS) is the most common material used for molding hydrogel structures [34–39]. PDMS molds are built using the photolithography technique, specifically soft lithography. In this technique, a light-sensitive material (photoresist) is used to create negative masks with micro-sized patterns previously designed in computer-aided design. The most popular photoresist is SU-8. The mixture of PDMS and curing agent is poured onto a mask. After solidification of the PDMS, it is removed from the mask [40]. The PDMS mold can be used as a stamp [36,37,39] or sealed on a substrate (glass or preoxidized PDMS) to create perfusable microchannels [34,35,38].

Zheng et al. [39] used a microstructured PDMS stamp to mold type I collagen through *in situ* injection and gelation of collagen with or without perivascular cells (human brain vascular pericytes (HBVPCs) and human umbilical arterial smooth muscle cells (HUASMCs)) in plexiglass jigs and sealing of two collagen layers to form the enclosed fluidic structure (100 $\mu\text{m} \times 100 \mu\text{m}$) by applying pressure within the final plexiglass device. The enclosed microstructure had an inlet and an outlet that enabled the seeding of ECs and perfusion of the vessels with medium during culture (Fig. 2A and B). Using this microfluidic vascular network, the authors elucidated the angiogenic activities of the endothelia (HUVECs injected into the microchannel) and the differential interactions with perivascular cells (HBVPCs and HUASMCs) seeded in the collagen. In a similar study, Trkov et al. [35] used perfusable PDMS microchannels to inject cell-suspended polymers to create micropattern hydrogels with encapsulated cells and to study the interactions between endothelial and mesenchymal cells that promote vasculogenesis (Fig. 2C). Fibrin hydrogel micropatterning allows these two cell populations to be spatially positioned at controllable channel-to-channel distances (500, 1000, or 2000 μm). Populations of human mesenchymal stem cells (hMSCs) from bone marrow, umbilical cord vein, and umbilical cord artery could migrate into fibrin hydrogel. However, only hMSCs from bone marrow presented migration rate dependence on the channel-to-channel distance from HUVECs, which was associated with chemokines secreted by HUVECs that stimulate the directional migration of MSCs and the formation of stable vascular networks. Fibrin micropatterning hydrogel was also used to mimic the sequential steps of angiogenic processes of neovessel formation: sprouting, elongation, and maturation by culturing pericytes together with ECs. EC-pericyte cocultured vessels reflected various pathophysiological conditions of microvessels *in vivo*, including the ability of pericytes to prevent enlargement of blood vessels, thereby stabilizing and helping ECs to establish a denser vascular network with more interconnecting junctions and branches [41]. Recently, PDMS molds and poly (N-isopropylacrylamide) (PNIPAM) fibers were used to generate microchannel networks of gelatin to contribute to the development of therapeutics for hypoxia/inflammation-related diseases, including ischemic limb disease. For this, the gelatin hydrogels were implanted in mouse and porcine models of hindlimb ischemia, followed by the infiltration of endothelial and RAW 234.7 cells from the distal site of the ischemic hindlimb to the implanted hydrogels. The microchannel hydrogel induced invasion and prohealing (M2) polarization of monocytes and thus promoted endothelial cell ingrowth from the host vessel side to localize into microchannels, leading to the facilitation of blood perfusion [42].

PDMS molds manufactured by soft lithography can also be used to produce sacrificial molds with patterned microchannels (Fig. 2D). The sacrificial molds are immersed in a prepolymer solution and then, after gel crosslinking, removed by dissolution in water [33], dissociation in chelating reacting solution [38] or heating [34]. Poly (vinyl alcohol) (PVA), calcium alginate, and gelatin have been used to produce perfusable vascular architectures in different hydrogels, followed by their endothelialization. In the obtained architectures, ECs grew, lined the channels, and proliferated to form vascular lumens [33,34,38]. Baker et al. [36] used gelatin as a sacrificial material to create collagen channels with different geometries. The microchannel patterning architectures

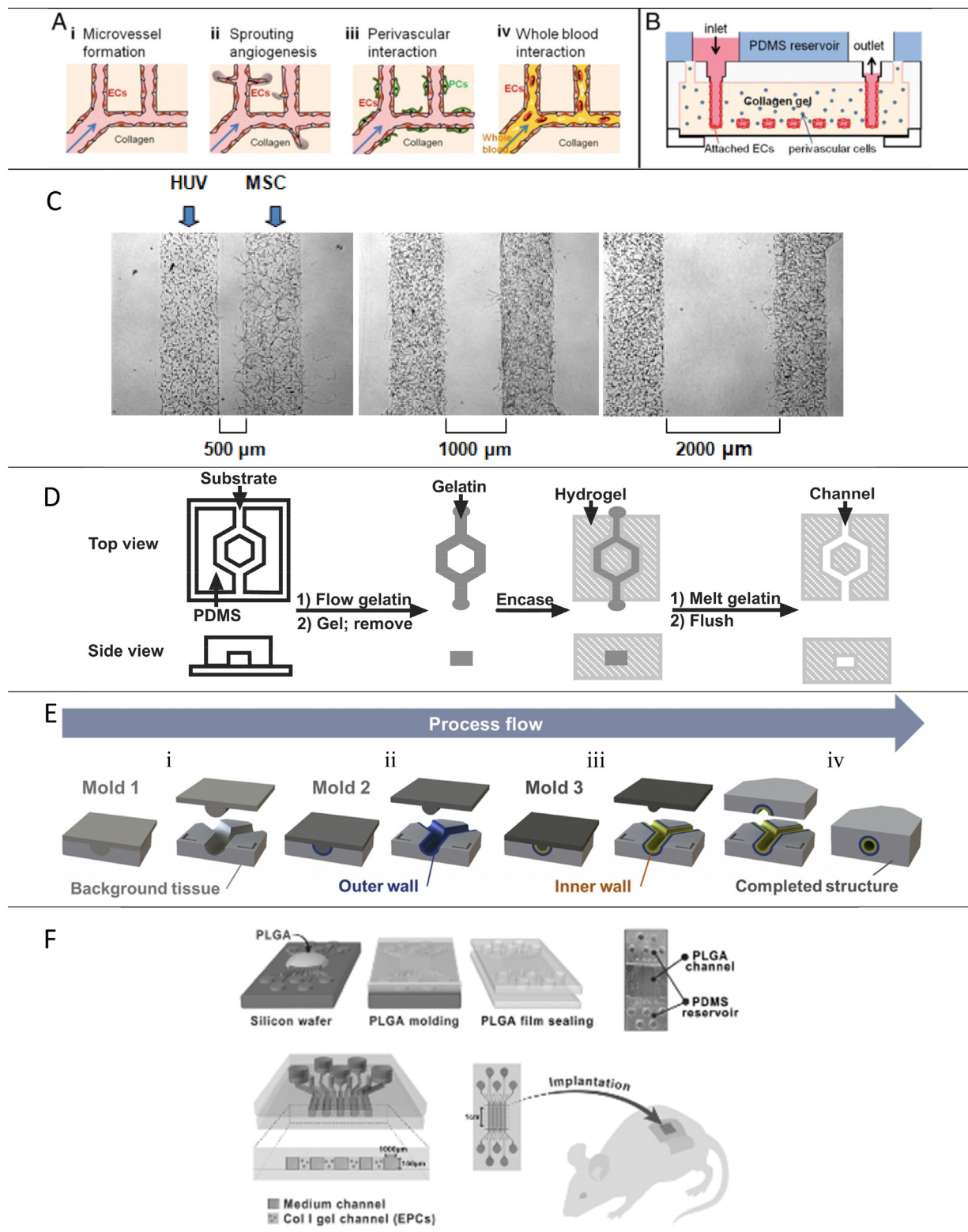


Fig. 2. A) Schematic diagram of the microfluidic vascular network illustrating (i) morphology and barrier function of endothelium, (ii) endothelial sprouting, (iii) perivascular association, and (iv) blood perfusion [39]. B) Schematic diagram of microfluidic collagen scaffolds after fabrication [39]. C) Micropatterned fibrin channels loaded with human umbilical vein endothelial cells (HUVECs; left channel) and mesenchymal stem cells (MSCs; right channel), with distances between channels of 500, 1000, and 2000 μm [35]. D) Schematic diagram of the manufacture of micropatterned hydrogels using a sacrificial material [34]. E) Fabrication method of multi-layered hydrogel microstructures loaded with cells using coaxial geometries. The first step (i) creates the background tissue; the second (ii) defines the outer vessel wall; the third (iii) defines the inner wall. The two molded halves of the final structure are then brought together (iv) and bond by further gelation [44]. F) Overall schematic illustration of poly (ethylene glycol) diacrylate (PEGDA) microfluidic device fabrication and implantation of the device seeded with human endothelial progenitor cells (hEPCs) [45].

allowed the generation of controllable spatial diffusive gradients of soluble angiogenic growth factors, guiding 3D morphogenetic processes such as endothelial sprouting.

Despite the potential use of the abovementioned vascular architectures in cell therapy and tissue engineering, these studies are preliminary and present some disadvantages to be overcome. Some sacrificial materials, such as gelatin and calcium alginate, are flexible, and they can distort within the prepolymer solution, which may result in microchannels that are not entirely identical [34]. In addition, most of the architectures are produced from rectangular cross-section molds, leading to rectangular tubular microchannels. These microchannels might result in nonphysiological flow dynamics for the cells [17]. A simple method of creating circular microchannels is to place a cylindrical mold, such as a needle or a rod, through the gel as it crosslinks. After the gel crosslinks, removal of the needles results in a hollow perfusable channel. Using two parallel acupuncture needles, Nguyen et al. [37] created two type I collagen perfusable tubes (diameter = 400 μm). One of the channels was then coated with ECs, and growth factor gradients were controllably created by perfusion through the channels. In a similar work, Nichol et al. [43] applied HUVECs to the microchannel entrance produced with GelMA; they were drawn in by capillary force. Cells readily adhered to, migrated within, proliferated, and organized both on 2D and 3D GelMA micropatterns. To provide a more physiological microenvironment for the cells, Heidari & Taylor [44] created multilayered hydrogel microstructures loaded with cells using coaxial geometries ranging from 200 to 2000 μm in diameter (Fig. 2E). The obtained architecture allowed us to establish direct contact between multiple types of cells, incorporating heterogeneous elastic modules to ensure the ideal growth and controllability of each produced layer's thickness, cell density, and composition. Vasculogenesis is also an important morphogenetic event for ischemic disease treatment. Kim et al. [45] developed an implantable poly (lactic-co-glycolic acid) (PLGA) microfluidic device to study the formation of three-dimensional (3D) vasculature by human endothelial progenitor cells (hEPCs) *in vivo*. This device was the first to be produced by the micromolding technique and implanted *in vivo* into athymic mice's subcutaneous space (Fig. 2F). When the microfluidic devices were retrieved one and four weeks after implantation, blood vessel formation was observed around the implanted PLGA devices, indicating that these implantable scaffolds may be useful for treating ischemic diseases.

2.2.2. Microfluidics

Microfluidic technology is used to precisely control and manipulate small quantities of fluids on microscale [46,47]. In addition, the use of microfluidics provides several benefits over macroscale encapsulation methods. The microscopic diameter of channels contributes to forming a laminar flow regime (low Reynolds numbers), enabling the generation of coaxial flow among multiple fluids that diffuse slowly and mix across the adjacent streams [31,48]. Thus, the characteristics of formed structures can be precisely changed by modulating fluid properties, microchannel design, and parameter processes, such as the flow rate of fluids. In addition, since low shear stress is applied, many sensitive biological materials, such as proteins, vectors, and cells, can be encapsulated without incurring significant damage [49–52].

A wide range of microfluidic devices have been produced using different techniques (laser ablation, micromachining, and soft lithography) and materials (glass, PDMS, quartz, silicon, and thermoplastic), with PDMS and glass-based microfluidic chips being the most commonly used [17,53]. Planar devices present channels with rectangular cross-sections that are easily designed and produced by soft lithography using PDMS, whereas microcapillary devices are assemblies of coaxial capillary tubes typically made with glass [54,55]. Microfluidics techniques have been applied to generate diverse microscale structures for cell encapsulation, mainly droplets and microfibers.

2.2.2.1. Microfibers. Microfibers have potential applications in vascular tissue engineering since they could be used *in vivo* to replace blood vessels and restore vascular function [56]. In microfluidics, microfibers are synthesized by solidifying the microflows containing the prepolymer fluid using photopolymerization or ion crosslinking treatment [57]. Usually, microcapillary devices are chosen to produce cell-laden microfibers due to their hydrophilic character and cylindrical cross-section, which favor the formation of stable laminar flows for controllable gelation and fine control over structure shape, size, chemical anisotropy, and biological activity [49,58].

Cheng et al. [59] developed a capillary-based coaxial microfluidic device to manufacture perfusable alginate microfibers that could be assembled with multiple layers to generate multi-shell and multi-hollow microfibers. In a typical experiment of developing microfluidic fibers, an alginate dispersion was pumped through the circular capillary as core flow, while calcium chloride was pumped in the same direction through the region between the inner circular capillary and the outer square capillary (Fig. 3A, B, and C). A co-focusing flow led to the formation of a 3D coaxial sheath around the alginate at the point of merging of both flows. Microfibers with highly uniform cylindrical shapes were generated *in situ* because of the rapid diffusion-controlled ion crosslinking; in addition, their diameters could be precisely adjusted by changing the core and sheath flow rates [59]. Liu et al. [56] used a similar microcapillary device (Fig. 3D) to assess for the first time the angiogenic growth factor released from alginate microfibers loaded with MSCs, the endothelial differentiation of the encapsulated cells, and the use of cell-laden microfibers in a subcutaneous implant *in vivo*. The encapsulated cells proliferated in the microfibers and presented stable endothelialization under the angiogenic effects of vascular endothelial growth factor and fibroblast growth factor. However, the *in vivo* implant indicated that the cell-laden microfibers caused a mild host reaction.

The biopolymer alginate has broad applicability as a candidate in creating microfibers due to its rapid gelation, an indispensable requirement in the microfluidic approach. However, some studies suggest poor biocompatibility of alginate, which could limit its biological applications. Diverse cells, such as fibroblasts and ECs, exhibit low viability while encapsulated in alginate fibers. In addition, clinical studies of alginate-encapsulated islet transplantation have resulted in strong fibrotic overgrowth around the microstructures [26,57]. Certain strategies have been applied to make use of the advantages and overcome the disadvantages of this biopolymer. Zuo et al. [57] demonstrated the preparation of alginate-GelMA composites for microfluidic fiber fabrication. The double coaxial flow microfluidic device comprised two adjacent cylindrical glass capillaries connected to a square glass capillary (Fig. 3E). Double-layer hollow microfibers were prepared to inject hyaluronic acid into the 1st inlet and the alginate-GelMA composite into the 2nd and 3rd inlets. Due to laminar effects, these fluids formed coaxial flows, and the alginate-based fluids quickly gelled when they reached the outlet composed of 100 mM CaCl_2 solution. GelMA gelation was induced by exposure to ultraviolet (UV) light outside the channel, and hyaluronic acid flowed out of the microfibers due to the inertia effect, leading to the formation of the perfusable channel in the microfibers. This approach offers great potential for application in different human tissues with complex structures, particularly blood channels, since the fibers proved to possess higher mechanical moduli, better stretching performance, and better cellular bioactivity than pure alginate [57].

2.2.2.2. Droplets. Microfluidics also offers a new approach to producing droplets, such as emulsion assembly [60]. Emulsion droplets are generated individually at the channel junction when viscous and interfacial forces exceed inertial forces [55,61]. T-, Y- and cross-junctions between the channels are the most common planar devices used for droplet production. In a cross-junction, the shear stress is imposed by the continuous

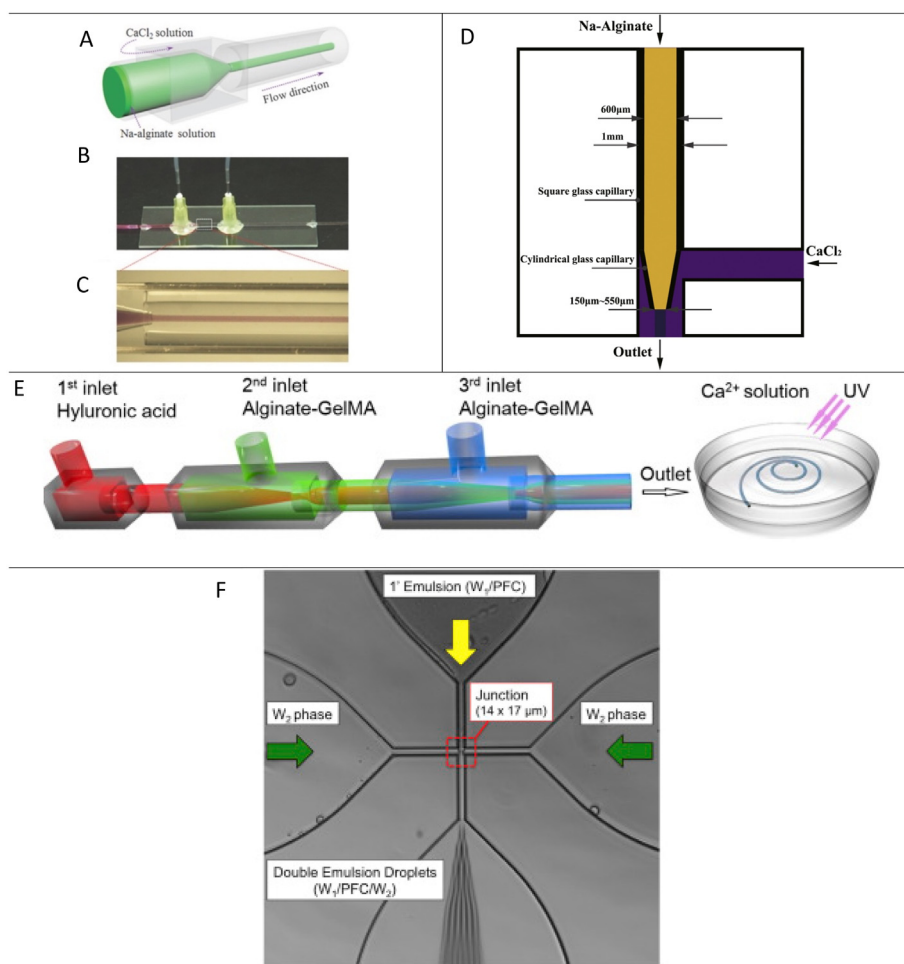


Fig. 3. A) Schematic illustration of the capillary coaxial microfluidic device used for microfiber production [59]. B, C) Digital photographs of the capillary device and its microstructure during the formation of the microfibers [59]. D) Schematics of microfiber generation apparatus and the principle of gelation [57]. E) Formation of double-layer hollow microfibers after Ca-alginate reaction and UV exposure [56]. F) Flow-focusing geometry of the quartz microfluidic device, including the $14 \times 17 \mu\text{m}$ junction where the monodispersed double emulsions were formed [63].

phase stream at both sides of the dispersed phase stream in a technique known as hydrodynamic flow-focusing, which leads to the generation of more uniform and smaller droplets as compared with those formed via T- or Y-junctions [55,62]. Monodisperse droplets used as delivery systems have more consistent release kinetics than the polydisperse droplets produced by conventional emulsification methods, such as high-pressure homogenization [55,63].

Tiemeijer et al. [64] used PDMS devices with a flow-focusing geometry to study the biological function of human monocyte-derived macrophages at single-cell resolution with high throughput. HFE oil was inserted into the microchannels via the outermost inlet, while cells and the thermoreversible polyisocyanide (PIC) with cytokines (LPS and IFN- γ for a proinflammatory M1 phenotype or IL-4 and IL-13 for a prohealing M2 phenotype) were inserted from the inner two inlets. After the desired culture period, the droplets were cooled, followed by de-emulsification, resulting in easy cell retrieval. Culturing single macrophages in PIC microbeads resulted in higher cell viability and enhanced M2 polarization than culturing single macrophages in suspension. However, co-encapsulating multiple cells enhanced cell polarization compared to single cells, since cells need paracrine factors produced by other cells to maintain their behavior and biological function. Thus, single-cell hydrogel-based systems proved to be quite suitable for basic research on cellular behavior in angiogenesis processes. However, effective application of this type of system as an alternative cell therapy does not present good prospects.

Moncion et al. [63] used a flow-focusing quartz microfluidic device to produce double emulsions (Fig. 3F). A water-in-oil single emulsion containing basic fibroblast growth factor (bFGF) in the aqueous phase (W_1) and perfluorocarbon (PFC) as the oily phase was previously

produced via sonication and then pumped through the inner channel. The inner flow channel converged at the junction with two lateral flow channels of an aqueous solution of Pluronic F68, the W_2 aqueous phase. Double emulsions (diameter = $13.9 \pm 0.04 \mu\text{m}$ and coefficient of variance = 4.5%) were formed in a collection vial with a bFGF encapsulation efficiency of $99.3 \pm 1.6\%$. The fibrin matrix was doped with this double emulsion to produce acoustically responsive scaffolds (ARSs). In this delivery system, megahertz-range ultrasound (US) was used to generate acoustic droplet vaporization, which caused vaporization of the PFC phase within the emulsion and expulsion of the encapsulated payload. The authors showed that monodispersed emulsions displayed better stability and more controlled bFGF release from ARSs than polydisperse emulsions. In addition, *in vivo* studies demonstrated that the controlled release of bFGF from an ARS exposed to the US increased perfusion and blood vessel formation compared to an ARS without the US.

Therefore, micromolding and microfluidics are versatile technologies that allow the study of angiogenic processes *in vitro* and *in vivo* and the development of complex encapsulation systems that can be used as potential treatments for ischemic diseases. Table S2 shows a comparison of biostructures produced by micromolding and microfluidics approaches (supplementary material).

2.3. 3D printing as a potential technology for therapeutic angiogenesis applications

3D printing is considered a versatile technique to fabricate various types of complex three-dimensional (3D) structures across research and industrial fields, including in regenerative medicine [65]. Natural or synthetic polymeric structures with predesigned patterns and geometries

can be printed in the presence or absence of cells to create 3D biological architectures [66,67]. Tissue-engineered 3D biostructures have shown technological potential for use in angiogenic therapy to treat ischemic diseases by manufacturing perfusable single vessel or patterned vascular network implants [65,66]. Upon implantation, the 3D-printed vascular structures enabled cell differentiation and survival, increased vascularization, and recovery of ischemic limbs [65,66]. The success of the final application of 3D constructions is the result of choices related to some previously mentioned factors, such as cell type and the material properties, as well as specific characteristics of 3D technology, such as the bioprinting approach, process parameters, and 3D-printed architecture [68]. This section and Table S3 (supplementary material) summarize the technological approach and features applied to newly engineered vasculature biostructures produced by different 3D-printing techniques, including inkjet, layer-by-layer and thermal extrusion, stereolithography or digital light processing, and photodegradation.

2.3.1. Patterned vascular network

Previous studies have demonstrated that branched capillary beds can be induced by injecting a variety of proangiogenic growth factors and gene therapy vectors [69,70] or by implanting cell-laden hydrogels [71, 72]. However, capillary beds may not be suitable for the clinical treatment of ischemia since perfusion recovery is slow and, consequently, can promote insufficient circulation; moreover, the resulting vasculature tends to be randomly organized, unlike native capillary networks [71, 72]. Thus, the main advantage of 3D printing is to manufacture vascular networks in a specific pattern with ECs and mural cells before *in vitro* implantation. 3D-printed structures might favor implanted cell performance, rapid migration, and integration with host cells to generate functional blood vessels [65,73–75].

Considering the complex structural nature of vascular networks and their multiple cell composition, Kolesky et al. [73] reported a new 3D-printing method to manufacture patterned vascular networks with different cells and polymers. An engineered biostructure was produced by sequential printing of 4 inks (PDMS, Pluronic F127, and two different cell-laden GelMA inks) by extrusion-based bioprinting using a layer-by-layer approach. This printing approach combines a fluid-dispensing system for extrusion with a three-axis motor control system for ink deposition, and it also relies on the mechanical and temporal properties of the polymer being printed [76,77]. Therefore, the polymer must present shear-thinning behavior, i.e., at the high shear rates applied through the nozzle, it must be fluid enough to facilitate extrusion and, after deposition, solid enough to support itself [77]. PDMS was used to print a high-aspect ratio border that surrounds each vascular construction to enable exploration of the chemical and rheological behavior of other polymers (Pluronic F127 and GelMa) to produce inks that were thermally responsive and covalently crosslinked by UV light. The differences in thermally reversible gelation obtained for the Pluronic F127 (solid-like at $T > 22\text{ }^{\circ}\text{C}$ and liquid-like at $T < 4\text{ }^{\circ}\text{C}$) and GelMA inks (liquid-like at $T > 22\text{ }^{\circ}\text{C}$ and solid-like at $T < 4\text{ }^{\circ}\text{C}$) allowed the printing of 1D-, 2D-, and 3D-patterned vascular networks (Fig. 4Ai, ii, iii). The printed biostructures illustrated the potential for creating perfusable channels with different diameters (100 μm –1 mm), which were altered on demand by changing the printing pressure, speed, or nozzle height. In the last step of this work, a complex and patterned structure with multiple materials and cells was constructed (Fig. 4Aiv, v) by the sequential deposition of the PDMS ink, followed by a thin layer of GelMA loaded with 10T1/2 fibroblasts (at $37\text{ }^{\circ}\text{C}$ and further cooled to $15\text{ }^{\circ}\text{C}$), Pluronic F127 ink, and then a layer of human neonatal dermal fibroblast (GFP-HNDF) cell-laden GelMA. After printing, the patterned vascular networks were encapsulated by depositing a pure GelMA ink at $37\text{ }^{\circ}\text{C}$, illuminated with a UV light source to crosslink the GelMA species within the bulk matrix cooled to $4\text{ }^{\circ}\text{C}$ to liquefy the Pluronic F127 printed and used as sacrificial material. The printed microvessels were endothelialized, and the viability of the encapsulated cells was investigated. The initial cell viability (0 days) of the network structure (70% for the HNDFs

and 61% for 10 T/12 cells) was lower than that of the control samples produced by casting cell-laden GelMA films (approximately 80%). These results were associated with the shear stress that the cells experienced during the printing process. However, the cell viability increased after 7 days (to 81% for the HNDFs and 82% for 10 T/12 cells), indicating that the 3D bioprinting approach was nondestructive to them [73].

Extrusion bioprinting is the most commonly used approach for printing patterned vascular networks [65,73,74,78]. However, its resolution is limited for some bioapplications. The minimum resolution of viscous printing material (i.e., $\sim 200\text{ }\mu\text{m}$ for collagen and matrix proteins) may inhibit the fabrication of capillary-sized vessels for microvasculature networks if the required microscale resolution is not achieved [78]. In addition, improvement in resolution resulting from changing the printing process parameters (pressure and nozzle diameter) is limited by the shear rate values [68]. As mentioned above, high shear stress reduces cell viability and can affect the formation of viable vessels [68,73]. Thus, an application of the extrusion printing technique for manufacturing microvasculature networks was suggested by Lee et al. [78]. The extrusion-based layer-by-layer approach was also used to print two parallel perfusable channels ($\sim 1\text{ mm}$) to create an adjacent microvasculature network ($\sim 10\text{ }\mu\text{m}$) through a maturation process. Initially, a printed layer of collagen precursor was polymerized, heated gelatin was printed in a straight pattern and solidified at room temperature, a mixture of fibrinogen, thrombin, and cells was deposited between the two pattern channels, and then several layers of collagen were placed on top of the entire structure (Fig. 4B). The biostructure was incubated, and the perfusable channels were obtained after gelatin liquefaction. The printed channels were connected to pumps, and cells in suspension were injected into the channels to create a cell lining. The cells (endothelial cells and fibroblasts) immobilized within the fibrin gel created microvasculature derived from the larger printed vascular channels by angiogenic and vasculogenic processes. The proliferation and migration rates of normal human lung fibroblasts (NHLFs) were higher than those of HUVECs, filling a large part of the collagen structure. However, HUVECs first formed the capillary network within the fibrin, and then the network became denser and uniform; thus, the capillaries grew toward the collagen space already filled with NHLFs. In these biostructures, a fine-tuned flow rate of media perfusion was necessary to balance the viability of the vascular network and angiogenesis [79].

A recent approach used mouse models of limb ischemia to evaluate the effects of implantation of 3D-printed vascular networks on perfusion recovery and function of ischemic tissue *in vivo*. Carrabba et al. [80] developed a novel pattern scaffold consisting of a layer-by-layer printed synthetic polymer (poly (ϵ -caprolactone); PCL or polylactic-co-glycolic acid; PLGA) covered by a layer of electrospun gelatin nanofibers to recapitulate the rudimentary morphology and mechanical environment of the extracellular matrix surrounding the femoral artery. Human adventitial pericytes (APCs) were used to functionalize the scaffold by promoting neovascularization or cell recruitment with the secretion of paracrine factors. Then, these scaffolds were used as a substrate to extrude a patterned layer of HUVEC-laden gelatin to increase their therapeutic effect. The cellularized pattern scaffolds were highly biocompatible and promoted *in vitro* proangiogenic responses by the cells, increasing VEGF and FGF expression. Posteriorly, the *in vivo* efficacy of the pattern scaffolds was assessed with respect to their implantation around the occluded femoral artery of the mouse. The bioengineered PLGA scaffold outperformed the PCL counterpart by accelerating limb blood flow recovery through the formation of arterioles with diameters $> 50\text{ }\mu\text{m}$.

3D printing based on a thermal extrusion approach was applied to generate vasculature patterned *in vitro* within a fibrin patch for engineering host vasculature *in vivo* [65]. The differences between layer-by-layer extrusion and thermal extrusion are the availability of materials and the temperatures applied during the printing process. In thermal extrusion, carbohydrates such as isomalt, glucose, sucrose, and dextran are used to produce glass molds. The high temperatures

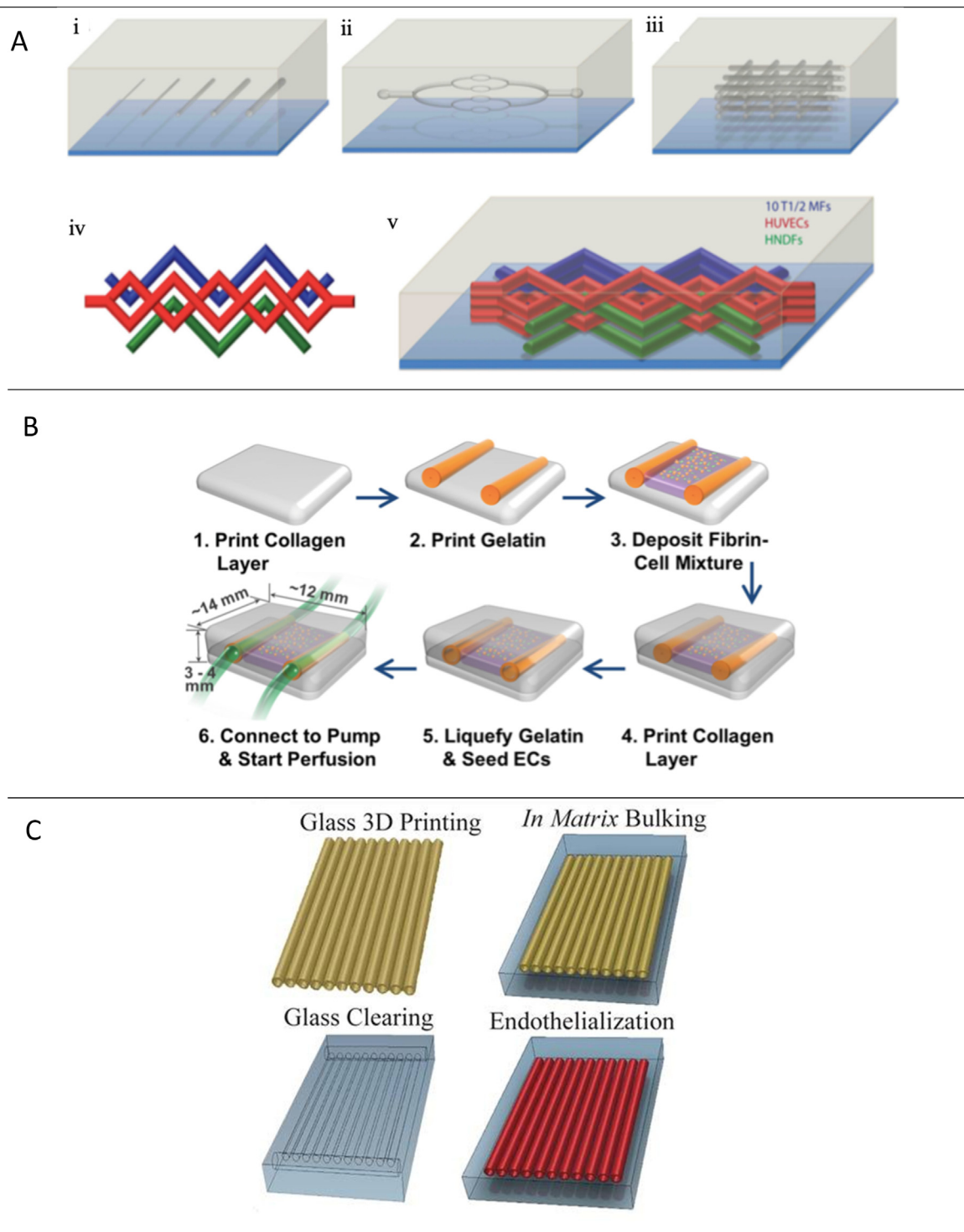


Fig. 4. (A) Schematic illustrations of 1D (i), 2D (ii), and 3D (iii) printed vascular networks and schematic views of the top-down (iv) and side (v) of the 3D construction printed with multi-materials and cells (blue, red, and green filaments correspond to printed 10T1/2 fibroblast-laden methacrylate gelatin (GelMA), Pluronic F127, and human neonatal dermal fibroblast cells (GFP-HNDF)-laden GelMA inks, respectively) [73]. (B) Channel construction and fibrin deposition procedure using 3D-printing extrusion-based on layer-by-layer approach [78]. (C) Schematic illustration of vascular patterned network fabrication by 3D-printing based on thermal extrusion [65]. (For interpretation of the references to color in this figure legend, the reader is referred to the Web version of this article.)

(approximately 110 °C) applied during the printing process prevent cells from being printed directly. Accordingly, the cells were seeded later [77]. Thus, to design vascular patches, sugar filaments (glass molds) composed of isomalt and dextran were printed in a network, the glass molds were encapsulated in a gel matrix, and the sugar was removed inside the channels by dissolution. Then, the ECs were injected to fill the channel

network (Fig. 4C) [65,74]. The authors showed that the architecture of the channels impacted the functionality of the implant and that its performance promoted circulation in that context. The presence of ECs without concomitant pattern organization into vascular structure fails to stabilize the circulation required to perfuse distal ischemic sites. Thus, implants with vessels patterned in a parallel geometry (200 μm diameter)

integrated with the host and rescued perfusion better than rescue observed with unpatterned or patterned implants in other geometries [65].

In another 3D-printed extrusion approach, wet-spun hydrogel fiber scaffolds were fabricated using a custom setup composed of a 3D-printed coaxial extruder placed centrally to the rotating Teflon drum connected to the stepper motor shaft. Skeletal muscle progenitors (human primary myoblasts or murine mesoangioblasts) were resuspended in the bioink and then extruded through the internal nozzle; a calcium chloride solution was extruded through the external nozzle. Bunched wet-spun fibers loaded with primary muscle precursors was implanted in the anterior muscle upon massive tibialis anterior (TA) ablation (~90% muscle mass removed). At 20 days after implantation, these constructs have shown an extraordinary capacity in regenerating muscle mass, vasculature, and innervation, thus allowing recovery of muscle functions [81].

As shown, extrusion-based 3D printing provides versatility and flexibility to build diverse and complex biostructures, necessarily involving a sacrificial material. The primary advantage of using Pluronic F127 and gelatin as sacrificial materials is their mild liquefying temperature; in addition, the latter is biocompatible and facilitates cell attachment, whereas sugar requires harsh solvents for removal [73]. Other challenges involved in this printing technique, such as the long-term structural stability of constructions and the occurrence of clogging and bursting during vascular network perfusion, may limit its use in large-scale production [75,82]. Alternatively, photodegradation is a light-based subtraction technique that involves the use of focused pulsed lasers with enough energy to break covalent bonds of photodegradable hydrogels to generate complex structures within them [83]. Heintz et al. [84] used this approach with image-guided laser control to create 3D vascular networks within poly (ethylene glycol) diacrylate (PEGDA) hydrogels, aiming to biomimic the natural architecture of *in vivo* vasculature. After degradation, monoacrylate poly (ethylene glycol)-RGDS was photocoupled to the PEGDA hydrogel, enabling cell adhesion to the channel surfaces (Fig. 5A). Thus, *in vitro* vascular networks lined with ECs were able to biomimic *in vivo* vasculature with high accuracy and resolution. The high resolution provided by precise light control allows the creation of patterned vascular networks; however, the use of high-energy laser light may raise concerns over its effects on cell integrity when it is already suspended in photodegradable hydrogel formulations [31,77].

Arakawa et al. [85] employed a multiphoton laser with cyto-compatible wavelengths and intensities to create multicellular 3D vascular networks. In this work, hydrogels were generated by cyto-compatible strain-promoted azide-alkyne cycloaddition between a poly (ethylene glycol) tetrabicyclononyne and a diazide-modified synthetic peptide (Fig. 5B and C). The peptide contained a photodegradable *ortho*-nitrobenzyl (oNB) linker and a matrix metalloproteinase cleavable sequence, which induced localized photolysis and allowed cell-mediated matrix remodeling, respectively. The channel network created within photosensitive gels presented a wide range of cross-sectional sizes (200 $\mu\text{m} \times 200 \mu\text{m}$, 100 $\mu\text{m} \times 100 \mu\text{m}$, 50 $\mu\text{m} \times 50 \mu\text{m}$, 25 $\mu\text{m} \times 25 \mu\text{m}$, and 10 $\mu\text{m} \times 10 \mu\text{m}$) that may cover almost all physiological vessel sizes of interest. In addition, the photodegradation printing approach was shown to be cyto-compatible for creating endothelialized microvascular networks with complex architectures in the presence of stromal cells suspended in hydrogel precursor formulation.

Manufacturing perfusable vascular networks by extrusion or laser-based bioprinters involves a serial “line by line” writing operation mode, which is time-consuming when used to fabricate complex structures and makes large-scale application unfeasible [75]. Thus, 3D printing based on projection stereolithography or digital light processing (DLP) has been adopted to fabricate complex 3D architectures, offering high speed and better print resolution, superior flexibility, and scalability (Fig. 6A). No physical masks or molds are needed. Instead, a digital micromirror device (DMD) chip can take digital 3D designs from a

computer and project them continuously through an array of millions of individually controllable reflective mirrors, allowing the patterning of light in entire 2D planes. The light projection induces photopolymerization of the polymer solution in a reservoir to create 3D-printed structures [75,82]. Zhang and Larsen [86] used an aqueous prepolymer solution composed of poly (ethylene glycol) diacrylate (PEGDA), a photoinitiator (lithium phenyl-2,4,6-trimethylbenzoylphosphine), and a photoabsorber (quinoline yellow) to produce square or circular channels smaller than 100 $\mu\text{m} \times 100 \mu\text{m}$ in width and height or 300 μm in diameter, respectively. Each layer of the patterned vascular network took less than 15 s to be photopolymerized, and then printed channels were functionalized with gelatin-based ligands to support cell attachment. The continuous advances in optical components developed for stereolithography projection printing make it suitable for producing complex 3D structures on a large scale with high resolution and speed. Xue et al. [82] printed complex structures with biomimetic irregular bifurcations and different channel sizes in less than 3 s using the DLP printing approach. The vascular networks, called arborescent and capillary networks, were composed of curved channels that bifurcated from the trunk (>1100 μm in width) to the small branch (~17 μm in width) (Fig. 6B and C). Cells were seeded into the trunk inlet of vascular networks until the channels were entirely filled. Clogging was observed at some small branches, caused by flow friction, which became significant when high-density cell solution encountered bifurcations. However, uniform cell distribution was achieved in the channels with a width larger than 30 μm , showing further attachment and penetration during cell culture proliferation.

Traditionally, stereolithography has been used to manufacture cell-free structures; however, a recent DLP approach allows direct printing of cell-laden materials since the projection minimizes the potential for cell damage by UV light [75]. Zhu et al. [75] suggested printing cells directly into the patterned vascular network without sacrificial material or perfusion to further simplify and speed up the printing process of biostructures. Structures with uniform channels and different channel widths (ranging from 50 μm to 250 μm) were used to encapsulate two different cell types, endothelial cells and fibroblasts, in the intended channels (red color) and the surrounding area (green color), respectively (Fig. 6D–I). The cell viability was higher (>85%) than that with respect to the biostructures obtained by 3D printing based on layer-by-layer extrusion since there was no negative influence of shear stress. The cells were exposed to UV light for less than 1 min during the printing process, which prevented their death. Fibroblast cells were induced into a pericyte phenotype to support the *in vitro* vessel formation mediated by ECs lining the channels. Additionally, a dense formation of the endothelial network and successful anastomosis between the patterned vascular network and the host vasculature were observed two weeks after *in vivo* implantation of the printed biostructure.

Despite the many advantages of applying 3D printing based on the DLP approach, avoiding overcuring other layers when starting gelation on the target layer is challenging. Thus, whereas the xy-axis resolution is improved by the DMD pixels, the z-axis resolution is low. The current strategy used to overcome this challenge is to use a photoabsorber that prevents undesired gelation and increases the resolution on the z-axis [31,86].

2.3.2. Perfusable single vessel

Although most 3D-printed patterned vascular networks have been developed with perfusable channels to achieve efficient integration and perfusion with the host vasculature, not all of these structures can be well anastomosed in a robust *in vivo* perfusion system. Thus, vascular implants containing a patterned network would be useful for a variety of ischemic conditions arising from microvasculature insufficiencies, such as diabetic wound healing and trauma such as burns and prophylaxis against the progression of poorly-perfused tissue. However, some lesions would

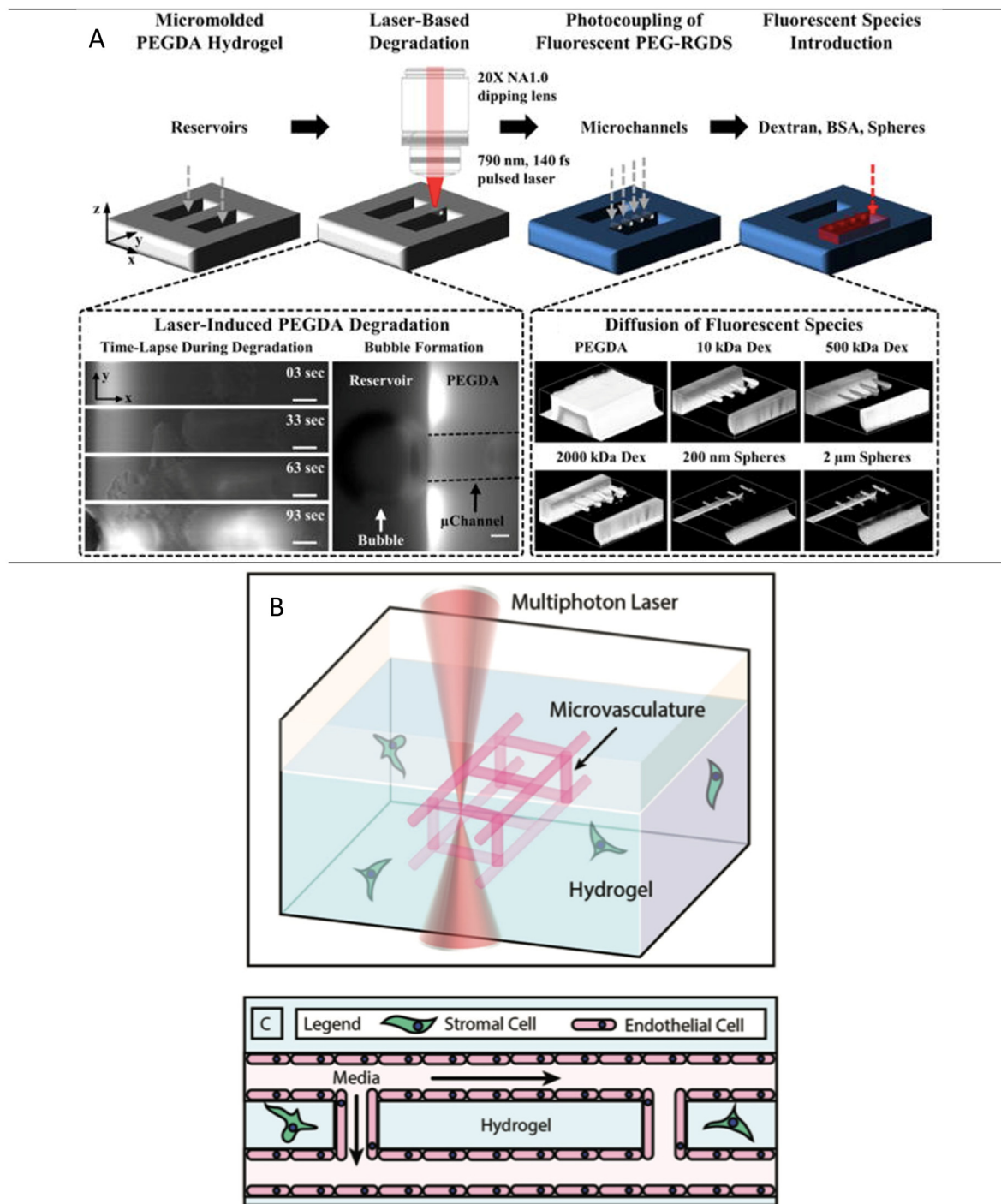


Fig. 5. A) Fabrication of patterned vascular networks in poly (ethylene glycol) diacrylate (PEGDA) hydrogels by 3D-printing based on photodegradation [84]. B) Multiphoton laser excitation induces localized degradation of the hydrogel through *ortho*-nitrobenzyl (*o*NB) photocleavage, resulting in the microchannel generation in the presence of encapsulated stromal cells [85]. C) Photodegraded microchannels were seeded with endothelial cells to create cell-laden hydrogels with perfusable vascular networks [85].

require replacing a large diseased vessel, which may involve the development of a perfusable single vessel to be applied as a graft for bypass surgery [65,66,87].

Perfusable single vessels were printed by extrusion based on a layer-by-layer approach using agarose as the sacrificial material [88,89]. Skardal et al. [89] used a bioprinter customized with a microcapillary tube to fabricate macrofilaments of agarose or cell-laden TetraPac13 (a cell-containing macrofilament). By selecting agarose or cell-containing macrofilaments at the appropriate point in the printing process, they

could deposit cells in a tubular orientation using agarose as a mold (Fig. 7A; B). The authors reported that the cells loaded into the perfusable single vessel (~500 μ m inner diameter) were viable for 4 weeks in culture. However, the system was inefficient because the printer had to be paused while microcapillary tubes in the printhead were switched manually during the bioprinting process. This drawback was overcome by Norotte et al. [88] through automation of the printing steps. First, cells were aggregated into discrete units, multicellular spheroids and cylinders. Then, they were printed concomitantly with agarose

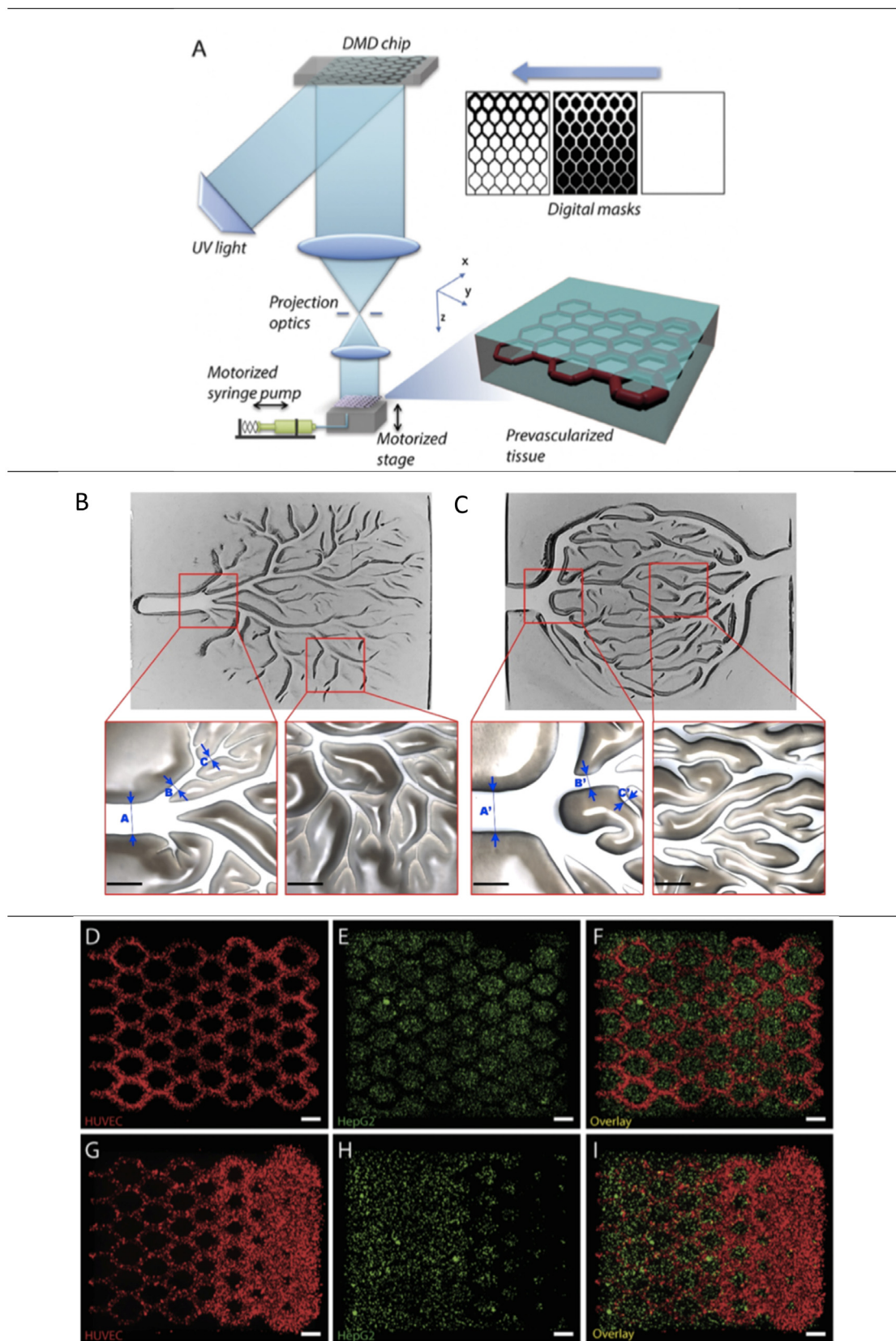


Fig. 6. (A) Schematic of the 3D-printing based on digital light processing. DMD: digital micromirror device [75]. Optical images of whole and details of printed (B) arborescent and (C) capillary network structures. In the zoomed images, the white regions are channels, and others are cross-linked poly (ethylene glycol) diacrylate (PEGDA). A, B, C and A', B', C' (in blue) are the measured position. Scale bar: 1 mm [82]. (D–I) Fluorescent images demonstrating the bioprinting of multi-cell-laden structures with uniform (D–F) and different channel widths (G–I). Endothelial cells (red) are encapsulated in the intended channels and fibroblast cells (green) are encapsulated in the surrounding area. Scale bars = 250 μm [75]. (For interpretation of the references to color in this figure legend, the reader is referred to the Web version of this article.)

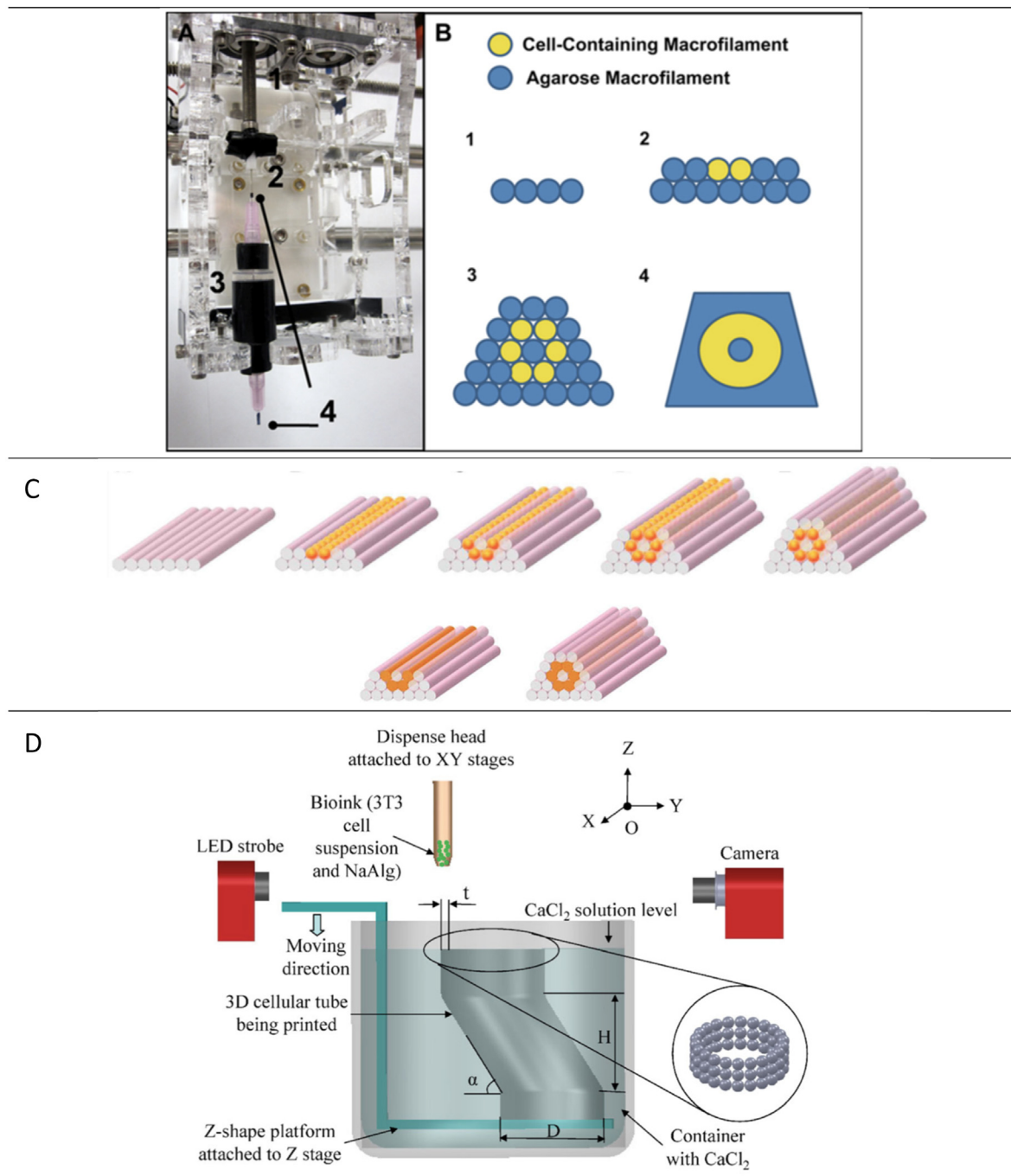


Fig. 7. A) Fab@Home printing system: 1. Syringe motor driveshaft; 2. Wire plunger inserted into the microcapillary tube; 3. The plastic adaptor which holds the microcapillary tube; and 4. The microcapillary tube [89]. B) Deposition scheme for printing a perfusable single-vessel, using agarose and cell-containing macrofilament [89]. C) Deposition scheme for printing a single-layered perfusable vessel of agarose macrofilament in pink and multicellular spheroids in orange [88]. D) Schematic of the proposed platform-assisted inkjet printing system by drop-on-demand (DOD) mode [90]. (For interpretation of the references to color in this figure legend, the reader is referred to the Web version of this article.)

macrofilaments using a printer equipped with two printheads, one for the preparation and extrusion of agarose macrofilaments and the other for the deposition of multicellular units in a fully automated cycle (Fig. 7C). The computer-aided motion and coordination of the two printheads assured the reproducibility of the preprogrammed pattern. Single- and double-layered perfusable vessels with outer diameter ranging from 0.9 to 2.5 mm were created after fusion of the discrete units mediated by cell–cell interactions. The fusion of the cellular cylinders was significantly more rapid (2–4 days) than that of spheroids (5–7 days), leading to the formation of uniform and nonuniform tubes, respectively. Similar to

other extrusion 3D-printing approaches, building these 3D structures is time-consuming, especially considering the preparation and fusion time of the multicellular units. In addition, removing the agarose macrofilaments by manually pulling them out of the tube was a procedure that challenged the structure's sterility and resolution. However, the use of no or an alternative (e.g., thermoreversible, photosensitive) sacrificial material would eliminate this disadvantage. Two 3D-printing approaches reported the construction of perfusable single vessels without using sacrificial material. In the first study, Xu et al. [90] used a platform-assisted inkjet printing system using the drop-on-demand

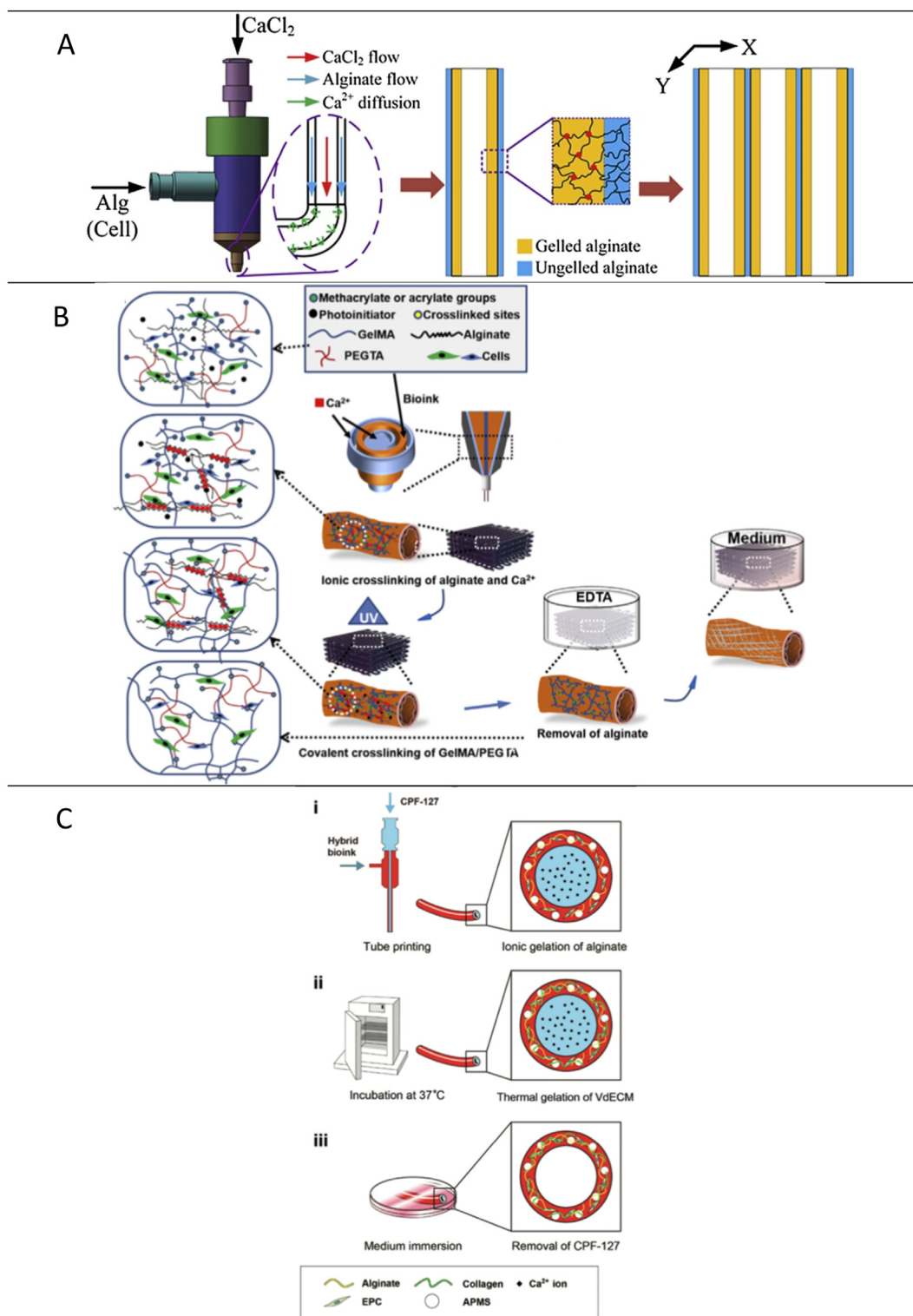


Fig. 8. A) Schematic experimental setup of the 3D-printing based on extrusion by coaxial nozzle approach [92]. B) Schematic diagram showing two independent crosslinking processes of the bioink, where alginate, methacrylate gelatin (GelMA), and poly (ethylene glycol)-tetra-acrylate (PEGTA) are ionically and covalently crosslinked, respectively, upon exposure to calcium chloride (CaCl₂) solution and UV light [93]. (C) Schematic diagram showing the perfusable single-vessel fabrication process: (i) ionic gelling of alginate contained in the hybrid bioink (vascular-tissue-derived decellularized extracellular (VdECM) and alginate), (ii) thermal crosslinking of collagen fibers induced by incubation at 37 °C, and (iii) immersion medium to remove Pluronic F-127 (CPF127) and obtain the tube [66].

(DOD) mode to fabricate tubes vertically through the fusion of alginate droplets with encapsulated fibroblast cells (Fig. 7D). Although the printed cell viability in the tubes was above 82% (or 93% with the control effect considered), this method was limited because it required the precise deposition of alginate droplets. In the second approach, 3D printing

based on extrusion by a coaxial nozzle approach allowed the fabrication of perfusable single vessels by extruding cell-laden material through a coupled core/shell nozzle (Fig. 8A) [91,92]. Human umbilical vein smooth muscle cells (HUVSMCs)-laden alginate and CaCl₂ solutions were extruded through the shell and core sections of the coaxial nozzle,

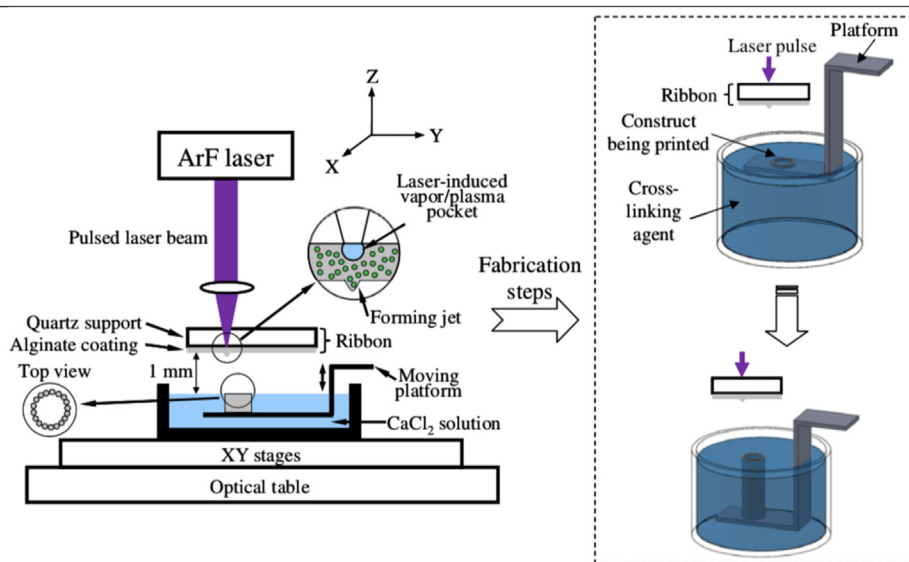


Fig. 9. Schematic diagram of experimental laser-assisted printing setup and manufacturing steps to print a perfusable single-vessel [94].

respectively. When these two materials came into contact, the alginate was ionically crosslinked by Ca^{2+} immediately [91]. The printed tube showed internal and external average diameters of approximately 990 μm and 1449 μm , respectively, and a length of 80 cm. However, although the single vessel was perfusable (no clogging or leakage), with burst pressures ranging between 43.24 and 303.73 mmHg, it could not support the burst pressure values of natural blood vessels (3561 mmHg). In addition, similar to other extrusion-based approaches, cell viability was substantially affected by the shear rate applied during printing (approximately 33%) and increased after 7 days of *in vitro* culture (to approximately 84%). Alginate is also the first biopolymer candidate to be used in the bioprinting approach due to its rapid gelation. However, alginate gels present deficiencies in terms of mechanical properties and binding sites for cell attachment and migration. These drawbacks have stimulated studies for partial alginate replacement with materials considered more biocompatible [66], and enabling its use only as a sacrificial material [93].

Jia et al. [93] used two independent crosslinking processes to produce a 3D-printed perfusable single vessel, where alginate was used as a sacrificial material. Alginate, GelMA, and poly (ethylene glycol)-tetraacrylate (PEGTA) were extruded through the shell nozzle. The ionic crosslinking of alginate was induced by complexation with Ca^{2+} delivery through the core nozzle and a CaCl_2 solution sprayed onto the outer surface of the tubes, which provided temporary structural stability during the bioprinting process (Fig. 8B). Covalent photocrosslinking of GelMA and PEGTA was subsequently induced by exposing the bioprinted construction to UV light, resulting in permanent fixation of its architecture. Then, the alginate was dissolved using a Ca^{2+} -chelating agent to provide better spreading and proliferation of the cells in the bioprinted construction. The tube's outer and inner diameters were modulated (50–1500 μm and 400–1000 μm , respectively) by changing the flow rates, moving speed, and/or switching on/off the bioink flow in the outermost channel of the printhead. After removing the alginate, the GelMA/PEGTA structure exhibited favorable biological characteristics that supported the spreading and proliferation of cells encapsulated in the structure, leading to the formation of biologically relevant, highly organized, perfusable vessels.

Only one study has assessed the potential use of the 3D-printed perfusable single vessel for the *in vivo* treatment of ischemic limb diseases. Gao et al. [66] produced a hybrid bioink from a mixture of vascular-tissue-derived decellularized extracellular matrix (VdECM) and

alginate to encapsulate EPCs and proangiogenic drugs (atorvastatin) in a perfusable single vessel obtained by 3D printing based on a coaxial nozzle approach and using Pluronic F-127 as a sacrificial material (Fig. 8C). The printed cell/drug-laden perfusable single vessel was transplanted into a nude mouse ischemic hindlimb without surgical anastomosis with the host blood vessels due to its weak mechanical properties. Despite this, the transplantation significantly reduced limb loss, foot necrosis, and toe loss compared to the control groups, and it also promoted blood perfusion and neovascularization in ischemia-injured sites in a ratio higher than the control groups.

As mentioned above, the weak mechanical strength of the perfusable single vessels hinders surgical anastomosis with the host blood vessel. This disadvantage may be overcome by designing a triple-coaxial nozzle to build a multilayer single vessel or increasing the polymer concentration. To our knowledge, no study has implemented the construction of multilayer single vessels, since this requires precise control of the gelation process, culture conditions of each layer and interactions between layers. In addition, increasing the polymer concentration can lead to nozzle clogging during the printing process due to its high viscosity. In this case, nozzle-free printing approaches are the most suitable for highly viscous polymers [94,95]. Yan et al. [94] built perfusable single vessels (nominal diameter of 3 mm) from highly viscous materials using a laser-assisted printing approach. The sodium alginate solution (2, 4, 6, and 8% w/v), which was coated on the bottom side of the quartz disc-based ribbon, was ejected due to the laser pulse-induced high-pressure bubble and deposited on the receiving platform inside the calcium chloride reservoir (Fig. 9). The sodium alginate concentration dominated the tube printing process when the laser fluence was low, and the laser fluence dominated when the sodium alginate concentration was low. Although the results presented are promising, the capacity of the printing technique and tubular structure to provide environmental conditions that allow viability, proliferation, and differentiation of cells remains unknown.

3. Perspectives and conclusions

This review discusses the most recent cell encapsulation technologies used to develop biostructures for treating ischemic diseases, with an emphasis on limb ischemia. All the advantages and limitations of each hydrogel-based encapsulation technology mentioned here are summarized in Table 1. Despite the potential application of these biostructures

Table 1
Advantages and limitations of hydrogel-based encapsulation technologies.

Technologies	Advantages	Limitations
Electrostatic droplet extrusion	<ul style="list-style-type: none"> - Production of small polymer droplets with controlled and uniform size under mild stress conditions (without using organic solvents and high temperatures). 	<ul style="list-style-type: none"> - Material restrictions and sterile operating conditions.
Micromolding	<ul style="list-style-type: none"> - Highly accurate control on channel sizes and xy-axis geometries. - High throughput, versatility, and reproducibility. 	<ul style="list-style-type: none"> - Rectangular cross-section molds lead to rectangular tubular microchannels. - Using flexible sacrifice material may result in non-identical microchannels. - It is hard to achieve z-axis channels. - It is hard to fabricate large-scale channel networks.
Microfluidics	<p>Fiber</p> <ul style="list-style-type: none"> - Laminar flow regime enables the generation of coaxial flow among multiple fluids. - Formation of continuous and stable flows for controllable gelation and fine control over structure shape and size. <p>Droplet</p> <ul style="list-style-type: none"> - Wide range of techniques and materials for microdevice production. - Production of small polymer droplets with controlled and uniform shape and size (highly monodisperse). - Versatility to produce different encapsulation systems. - Low shear stress. - Low cost. - Can integrate multiple nozzles to synchronously print cells and single/multiple materials with essentially no restrictions on the geometric complexity of the spatial arrangement. <p>Extrusion</p>	<ul style="list-style-type: none"> - Flow friction may affect fiber structure. - Clogging in microchannels. - Low droplet production rate. - It is hard to produce on a large-scale. - Flow of high viscosity materials. - Precise deposition of droplets. - Non-uniform droplet size. - Limited to low viscosity materials. - Shear stress can affect early cell viability. - Nozzle clogging. - Slow speed.
3D printing	<p>Inkjet</p>	

Table 1 (continued)

Technologies	Advantages	Limitations
	<ul style="list-style-type: none"> - Allowed to manufacture patterned vascular networks with different cells and polymers. - High cell density - Possibility of working with highly viscous materials 	<ul style="list-style-type: none"> - The material must present shear-thinning behavior. - Limited resolution, especially for the z-axis. - Shear stress can affect early cell viability. - Occurrence of clogging and bursting during perfusion.
	<p>Photodegradation</p> <ul style="list-style-type: none"> - High resolution. - Low shear stress. - Possibility of working with highly viscous materials. 	<ul style="list-style-type: none"> - High-energy laser light may cause cell damage. - "Line by line" writing operation mode is time-consuming when used to fabricate complex structures and makes large-scale applications unfeasible.
	<p>Digital light processing (DLP)</p> <ul style="list-style-type: none"> - High print speed. - High resolution. - Flexible and scalable printing process. - High cell density. - Projection minimizes the potential for cell damage. 	<ul style="list-style-type: none"> - High cost. - Occurrence of clogging in small channels (<30 μm). - Limited UV-light exposure times in cell-based systems. - Over-curing of non-target layers. - Low z-axis resolution.

in *ex vivo* gene and cell therapies and tissue engineering, the studies are preliminary, mainly involving *in vitro* and *in vivo* assays, and present several issues to be further investigated.

Hydrogel-based encapsulation systems must provide an adequate microenvironment to maintain the metabolic activity and viability of the immobilized cells. At the same time, they must offer suitable mechanical and temporal performance for the success of angiogenic therapy. Thus, the chosen encapsulation technology must allow precise control of the final biostructure density, morphology, porosity, and size. In some encapsulation approaches, cells can also experience high shear stresses, leading to reduced viability or death. To maintain cell integrity during and after cell encapsulation, a fine adjustment of prepolymer properties and applied shear rates is fundamental. In general, only cell viability is tested soon after encapsulation, but it is important to assess it for a longer period and to analyze relevant cell surface and gene expression markers to ensure that original properties remain. All of these points are very important for cell encapsulation because the cells confined within a small space are in contact with biopolymers and solutions, which are very different from their original environment.

Easy and fast fabrication processes with scalable production are aspects that must be considered for the transition from bench to clinical application. Electrostatic droplet generation has been the most tested technology *in vivo* since alginate is a fast-gelling material, and hMSCs are relatively easy to obtain. These factors are associated with the development of commercial equipment that ensures sterile conditions for encapsulating cells in a more efficient, reproducible, and controlled manner and potentiate the use of these systems in future clinical trials. In these trials, electrostatically generated cell-laden microbeads can be

administered via local injection according to conventional methods; however, hydrogel-based cell encapsulation could avoid many side effects associated with direct cell injection. Despite this technological potential, alginate's poor biocompatibility and degradation rate could limit its biological potential. Thus, more studies should be carried out to overcome the restrictions of fast gelling materials - an essential characteristic for developing hydrogel-based systems using electrostatic droplet generation technology.

The rapid restoration of blood flow to ischemic tissues is also essential for the progress of limb ischemia treatment, avoiding detrimental inflammation and other side effects. Versatile systems based on hydrogels produced by micromolding and microfluidic technologies were mainly implanted into the abdomens or dorsa of mice, aiming to study angiogenic activities of cells and growth factors *in vivo*. Despite the success of forming blood vessel structures in implants, further studies should focus on the proof-of-concept in animal models of limb ischemia. To make these studies viable, including clinical trials, the fabrication processes of hydrogel-based systems produced by micromolding and microfluidic technologies should require simple steps and be inexpensive and scalable. Most of the 3D bioprinting approaches presented here offer great potential for scalability and geometric/size adaptation of hydrogel-based systems. These features can make it possible to translate *in vivo* trials from small animal models to large animal models (such as swine, pigs, baboons, or dogs) and then into human clinical trial. Large-size animal model studies should address technological aspects related to (i) the surgical methods of connecting implants to host vessels, (ii) the possibility of fabricating hydrogel-based structures that adjust to the size of the animal, and (iii) the adjustment of gel stiffness to withstand the animal's physiological pressure.

It is important to highlight that although many hydrogel approaches have achieved excellent preclinical results, there are only few FDA-approved products for treating limb ischemia. Thus, regulatory approval is the main challenge in translating the hydrogel strategy from the laboratory to the clinic [96]. Finally, the technologies for genetic engineering, including gene-editing technology with Crispr-Cas9 to promote or inhibit the expression of specific proteins and iPSC (induced pluripotent stem cell) technology for providing any type of human and other animal cells, are potential tools to be associated with cell encapsulation technologies due to their ability to overcome the lack of a specific cell-type source and to serve as the means to produce these cells on a large scale for animal and human experiments.

Declaration of competing interest

The authors declare that they have no known competing financial interests or personal relationships that could have appeared to influence the work reported in this paper.

Acknowledgments

Ana Letícia Rodrigues Costa Leles is a recipient of the postdoctoral fellowship of the São Paulo Research Foundation (FAPESP) (grant #2020/02313-0). Sang Won Han and Lucimara Gaziola de la Torre are recipients of the fellowship of National Council for Scientific and Technological Development (CNPq) research productivity (303646/2019-5, 302212/2019-1). This project was funded by FAPESP (2015/20206-8, 2018/06635-1, and 2018/19537-8).

Appendix A. Supplementary data

Supplementary data to this article can be found online at <https://doi.org/10.1016/j.mtbio.2022.100221>.

References

- [1] L. Norgren, W.R. Hiatt, J.A. Dormandy, M.R. Nehler, K.A. Harris, F.G.R. Fowkes, Inter-society consensus for the management of peripheral arterial disease (TASC II), *J. Vasc. Surg.* 45 (2007) S5–S67, <https://doi.org/10.1016/j.jvs.2006.12.037>.
- [2] P. Libby, J.E. Buring, L. Badimon, G.K. Hansson, J. Deanfield, M.S. Bittencourt, L. Tokgozöglü, E.F. Lewis, Atherosclerosis, *Nat. Rev. Dis. Prim.* 5 (2019) 56, <https://doi.org/10.1038/s41572-019-0106-z>.
- [3] S.W. Han, C.A. Vergani Junior, P.E.O. Reis, Terapia gênica de isquemia de membro é uma realidade? *J. Vasc. Bras.* 19 (2020) <https://doi.org/10.1590/1677-5449.190059>.
- [4] P. Carmeliet, Mechanisms of angiogenesis and arteriogenesis, *Nat. Med.* 6 (2000) 389–395, <https://doi.org/10.1038/74651>.
- [5] F. Biscetti, N. Bonadia, E. Nardella, A.L. Cecchini, R. Landolfi, A. Flex, The role of the stem cells therapy in the peripheral artery disease, *Int. J. Mol. Sci.* 20 (2019), <https://doi.org/10.3390/ijms20092233>.
- [6] S. Braun, in: D. Duan, J.R. Mendell (Eds.), Non-viral Vector for Muscle-Mediated Gene Therapy BT - Muscle Gene Therapy, Springer International Publishing, Cham, 2019, pp. 157–178, https://doi.org/10.1007/978-3-030-03095-7_9.
- [7] T.R. Brazelton, M. Nystrom, H.M. Blau, Significant differences among skeletal muscles in the incorporation of bone marrow-derived cells, *Dev. Biol.* 262 (2003) 64–74, [https://doi.org/10.1016/S0012-1606\(03\)00357-9](https://doi.org/10.1016/S0012-1606(03)00357-9).
- [8] R.S. Stillhano, J.L. Madrigal, K. Wong, P.A. Williams, P.K.M. Martin, F.S.M. Yamaguchi, V.Y. Samoto, S.W. Han, E.A. Silva, Injectable alginate hydrogel for enhanced spatiotemporal control of lentivector delivery in murine skeletal muscle, *J. Contr. Release* 237 (2016) 42–49, <https://doi.org/10.1016/j.jconrel.2016.06.047>.
- [9] D. Seliktar, Designing cell-compatible hydrogels for biomedical applications, *Science* 336 (2012) 1124–1128, <https://doi.org/10.1126/science.1214804>.
- [10] F.H. Gage, Cell therapy, *Nature* 392 (1998) 18–24, https://www.unboundmedicine.com/medline/citation/9579857/Cell_therapy_.
- [11] J. Wan, Microfluidic-based Synthesis of Hydrogel Particles for Cell Microencapsulation and Cell-Based Drug Delivery, 2012, <https://doi.org/10.3390/polym4021084>. *Polymers* (Basel).
- [12] F.S. Palumbo, S. Federico, G. Pitarresi, C. Fiorica, G. Giammona, Gellan gum-based delivery systems of therapeutic agents and cells, *Carbohydr. Polym.* (2020), <https://doi.org/10.1016/j.carbpol.2019.115430>.
- [13] T. Andersen, P. Auk-Emblem, M. Dornish, 3D Cell Culture in Alginate Hydrogels, *Microarrays*, 2015, <https://doi.org/10.3390/microarrays4020133>.
- [14] A. Murua, M. de Castro, G. Orive, R.M. Hernández, J.L. Pedraz, In vitro characterization and in vivo functionality of erythropoietin-secreting cells immobilized in Alginate–Poly-L-Lysine–Alginate microcapsules, *Biomacromolecules* 8 (2007) 3302–3307, <https://doi.org/10.1021/bm070194b>.
- [15] E.S. Chan, B.B. Lee, P. Ravindra, D. Poncellet, Prediction models for shape and size of calcium-alginate macrobeads produced through extrusion-dripping method, *J. Colloid Interface Sci.* (2009), <https://doi.org/10.1016/j.jcis.2009.05.027>.
- [16] R. Yao, R. Zhang, X. Wang, Design and evaluation of a cell microencapsulating device for cell assembly technology, *J. Bioact. Compat. Polym.* (2009), <https://doi.org/10.1177/0883911509103329>.
- [17] H. Kim, C. Bae, Y.M. Kook, W.G. Koh, K. Lee, M.H. Park, Mesenchymal stem cell 3D encapsulation technologies for biomimetic microenvironment in tissue regeneration, *Stem Cell Res. Ther.* (2019), <https://doi.org/10.1186/s13287-018-1130-8>.
- [18] V. Manojlovic, J. Djonlagic, B. Obradovic, V. Nedovic, B. Bugarski, Immobilization of cells by electrostatic droplet generation: a model system for potential application in medicine, *Int. J. Nanomed.* (2006), <https://doi.org/10.2147/nano.2006.1.2.163>.
- [19] W. Zhang, X. He, Encapsulation of living cells in small (~100 μm) alginate microcapsules by electrostatic spraying: a parametric study, *J. Biomech. Eng.* (2009), <https://doi.org/10.1115/1.3153326>.
- [20] H.R. Moyer, R.C. Kinney, K.A. Singh, J.K. Williams, Z. Schwartz, B.D. Boyan, Alginate microencapsulation technology for the percutaneous delivery of adipose-derived stem cells, *Ann. Plast. Surg.* (2010), <https://doi.org/10.1097/SAP.0b013e3181d37713>.
- [21] S.K. Leslie, D.J. Cohen, J. Sedlacek, E.J. Pinsker, B.D. Boyan, Z. Schwartz, Controlled Release of Rat Adipose-Derived Stem Cells from Alginate Microbeads, *Biomaterials*, 2013, <https://doi.org/10.1016/j.biomaterials.2013.07.017>.
- [22] N. Landázuri, R.D. Levit, G. Joseph, J.M. Ortega-Legaspi, C.A. Flores, D. Weiss, A. Sambanis, C.J. Weber, S.A. Safley, W.R. Taylor, Alginate microencapsulation of human mesenchymal stem cells as a strategy to enhance paracrine-mediated vascular recovery after hindlimb ischaemia, *J. Tissue Eng. Regen. Med.* (2016), <https://doi.org/10.1002/term.1680>.
- [23] D.A. Kedziorek, L.V. Hofmann, Y. Fu, W.D. Gilson, K.M. Cosby, B. Kohl, B.P. Barnett, B.W. Simons, P. Walczak, J.W.M. Bulte, K. Gabrielson, D.L. Kraitchman, X-ray-visible microcapsules containing mesenchymal stem cells improve hind limb perfusion in a rabbit model of peripheral arterial disease, *Stem Cell.* (2012), <https://doi.org/10.1002/stem.1096>.
- [24] F.E. Ludwinski, A.S. Patel, G. Damodaran, J. Cho, J. Furnston, Q. Xu, S.N. Jayasinghe, A. Smith, B. Modarai, Encapsulation of macrophages enhances their retention and angiogenic potential, *Npj Regen. Med.* (2019), <https://doi.org/10.1038/s41536-019-0068-5>.

- [25] P.H. Kim, H.G. Yim, Y.J. Choi, B.J. Kang, J. Kim, S.M. Kwon, B.S. Kim, N.S. Hwang, J.Y. Cho, Injectable multifunctional microgel encapsulating outgrowth endothelial cells and growth factors for enhanced neovascularization, *J. Contr. Release* (2014), <https://doi.org/10.1016/j.jconrel.2014.05.010>.
- [26] Y. Fu, C.R. Weiss, D.A. Kedziorok, Y. Xie, E. Tully, S.M. Shea, M. Solaiyappan, T. Ehtiati, K. Gabrielson, F.H. Wacker, J.W.M. Bulte, D.L. Kraitchman, Noninvasive monitoring of allogeneic stem cell delivery with dual-modality imaging-visible microcapsules in a rabbit model of peripheral arterial disease, *Stem Cell. Int.* (2019), <https://doi.org/10.1155/2019/9732319>.
- [27] N. Attia, E. Santos, H. Abdelmouty, S. Arafa, N. Zohdy, R.M. Hernández, G. Orive, J.L. Pedraz, Behaviour and ultrastructure of human bone marrow-derived mesenchymal stem cells immobilised in alginate-poly-L-lysine-alginate microcapsules, *J. Microencapsul.* (2014), <https://doi.org/10.3109/02652048.2014.898706>.
- [28] Y.H. Choi, S.H. Kim, I.S. Kim, K.M. Kim, S.K. Kwon, N.S. Hwang, Gelatin-based micro-hydrogel carrying genetically engineered human endothelial cells for neovascularization, *Acta Biomater.* (2019), <https://doi.org/10.1016/j.actbio.2019.01.057>.
- [29] J. Shen, Y. Ji, M. Xie, H. Zhao, W. Xuan, L. Yin, X. Yu, F. Xu, S. Su, J. Nie, Y. Xie, Q. Gao, H. Ma, X. Ke, Z. Shi, J. Fu, Z. Liu, Y. He, M. Xiang, Cell-modified bioprinted microspheres for vascular regeneration, *Mater. Sci. Eng. C* 112 (2020) 110896, <https://doi.org/10.1016/j.msec.2020.110896>.
- [30] Business Communication LCC, BUCHI B-395 Pro encapsulator, URL: <https://www.bcluae.com/encapsulator>, 12 October 2021, (n.d.). <https://www.bcluae.com/encapsulator> (accessed October 12, 2021).
- [31] R. Xie, W. Zheng, L. Guan, Y. Ai, Q. Liang, Engineering of Hydrogel Materials with Perfusable Microchannels for Building Vascularized Tissues, 2020, <https://doi.org/10.1002/sml.201902838>. Small.
- [32] K.M. Chrobak, D.R. Potter, J. Tien, Formation of perfused, functional microvascular tubes in vitro, *Microvasc. Res.* (2006), <https://doi.org/10.1016/j.mvr.2006.02.005>.
- [33] A. Tocchio, M. Tamplenizza, F. Martello, I. Gerges, E. Rossi, S. Argenti, S. Rodighiero, W. Zhao, P. Milani, C. Lenardi, Versatile Fabrication of Vascularizable Scaffolds for Large Tissue Engineering in Bioreactor, *Biomaterials*, 2015, <https://doi.org/10.1016/j.biomaterials.2014.12.031>.
- [34] A.P. Golden, J. Tien, Fabrication of microfluidic hydrogels using molded gelatin as a sacrificial element, *Lab Chip* (2007), <https://doi.org/10.1039/b618409j>.
- [35] S. Trkov, G. Eng, R. Di Liddo, P.P. Parnigotto, G. Vunjak-Novakovic, Micropatterned three-dimensional hydrogel system to study human endothelial-mesenchymal stem cell interactions, *J. Tissue Eng. Regen. Med.* (2010), <https://doi.org/10.1002/term.231>.
- [36] B.M. Baker, B. Trappmann, S.C. Stapleton, E. Toro, C.S. Chen, Microfluidics embedded within extracellular matrix to define vascular architectures and pattern diffusive gradients, *Lab Chip* (2013), <https://doi.org/10.1039/c3lc50493j>.
- [37] D.H.T. Nguyen, S.C. Stapleton, M.T. Yang, S.S. Cha, C.K. Choi, P.A. Galie, C.S. Chen, Biomimetic model to reconstitute angiogenic sprouting morphogenesis in vitro, *Proc. Natl. Acad. Sci. U. S. A.* (2013), <https://doi.org/10.1073/pnas.1221526110>.
- [38] X.Y. Wang, Z.H. Jin, B.W. Gan, S.W. Lv, M. Xie, W.H. Huang, Engineering interconnected 3D vascular networks in hydrogels using molded sodium alginate lattice as the sacrificial template, *Lab Chip* (2014), <https://doi.org/10.1039/c4lc00069b>.
- [39] Y. Zheng, J. Chen, M. Craven, N.W. Choi, S. Totorica, A. Diaz-Santana, P. Kermani, B. Hempstead, C. Fischbach-Teschl, J.A. López, A.D. Stroock, In Vitro Microvessels for the Study of Angiogenesis and Thrombosis, *Proc. Natl. Acad. Sci. U. S. A.*, 2012, <https://doi.org/10.1073/pnas.1201240109>.
- [40] A.P. McGuigan, D.A. Bruzewicz, A. Glavan, M. Butte, G.M. Whitesides, Cell encapsulation in sub-mm sized gel modules using replica molding, *PLoS One* (2008), <https://doi.org/10.1371/journal.pone.0002258>.
- [41] J. Kim, M. Chung, S. Kim, D.H. Jo, J.H. Kim, N.L. Jeon, Engineering of a biomimetic pericyte-covered 3D microvascular network, *PLoS One* (2015), <https://doi.org/10.1371/journal.pone.0133880>.
- [42] J.B. Lee, D.-H. Kim, J.-K. Yoon, D.B. Park, H.-S. Kim, Y.M. Shin, W. Baek, M.-L. Kang, H.J. Kim, H.-J. Sung, Microchannel network hydrogel induced ischemic blood perfusion connection, *Nat. Commun.* 11 (2020) 615, <https://doi.org/10.1038/s41467-020-14480-0>.
- [43] J.W. Nichol, S.T. Koshy, H. Bae, C.M. Hwang, S. Yamanlar, A. Khademhosseini, Cell-laden Microengineered Gelatin Methacrylate Hydrogels, *Biomaterials*, 2010, <https://doi.org/10.1016/j.biomaterials.2010.03.064>.
- [44] H. Heidari, H. Taylor, Multilayered microcasting of agarose–collagen composites for neurovascular modeling, *Bioprinting* 17 (2020) e00069, <https://doi.org/10.1016/j.bprint.2019.e00069>.
- [45] J. Kim, K. Yang, H.J. Park, S.W. Cho, S. Han, Y. Shin, S. Chung, J.H. Lee, Implantable microfluidic device for the formation of three-dimensional vasculature by human endothelial progenitor cells, *Biotechnol. Bioeng.* (2014), <https://doi.org/10.1002/s12257-014-0021-9>.
- [46] G.M. Whitesides, The origins and the future of microfluidics, *Nature* (2006), <https://doi.org/10.1038/nature05058>.
- [47] W.M. Saltzman, W.L. Olbricht, Building drug delivery into tissue engineering, *Nat. Rev. Drug Discov.* (2002), <https://doi.org/10.1038/nrd744>.
- [48] X. Mu, Q. Liang, P. Hu, K. Ren, Y. Wang, G. Luo, Laminar flow used as “liquid etch mask” in wet chemical etching to generate glass microstructures with an improved aspect ratio, *Lab Chip* (2009), <https://doi.org/10.1039/b904769g>.
- [49] Y. Jun, E. Kang, S. Chae, S.H. Lee, Microfluidic spinning of micro- and nano-scale fibers for tissue engineering, *Lab Chip* (2014), <https://doi.org/10.1039/c3lc51414e>.
- [50] S.J. Shin, J.Y. Park, J.Y. Lee, H. Park, Y.D. Park, K.B. Lee, C.M. Whang, S.H. Lee, On the fly” continuous generation of alginate fibers using a microfluidic device, *Langmuir* (2007), <https://doi.org/10.1021/la700818q>.
- [51] J.L. Madrigal, R.S. Stilhano, C. Siltanen, K. Tanaka, S.N. Rezvani, R.P. Morgan, A. Revzin, S.W. Han, E.A. Silva, Microfluidic generation of alginate microgels for the controlled delivery of lentivectors, *J. Mater. Chem. B* 4 (2016) 6989–6999, <https://doi.org/10.1039/C6TB02150F>.
- [52] V.D.P. Cinel, T.B. Taketa, B.G. de Carvalho, L.G. de la Torre, L.R. de Mello, E.R. da Silva, S.W. Han, Microfluidic encapsulation of nanoparticles in alginate microgels gelled via competitive ligand exchange crosslinking, *Biopolymers* 112 (2021), e23432, <https://doi.org/10.1002/bip.23432>.
- [53] H. Becker, C. Gärtner, Polymer microfabrication methods for microfluidic analytical applications, *Electrophoresis* (2000), [https://doi.org/10.1002/\(SICI\)1522-2683\(20000101\)21:1<12::AID-ELPS12>3.0.CO;2-7](https://doi.org/10.1002/(SICI)1522-2683(20000101)21:1<12::AID-ELPS12>3.0.CO;2-7).
- [54] W.J. Duncanson, T. Lin, A.R. Abate, S. Seiffert, R.K. Shah, D.A. Weitz, Microfluidic synthesis of advanced microparticles for encapsulation and controlled release, *Lab Chip* (2012), <https://doi.org/10.1039/c2lc21164e>.
- [55] A.L.R. Costa, A. Gomes, R.L. Cunha, Studies of droplets formation regime and actual flow rate of liquid-liquid flows in flow-focusing microfluidic devices, *Exp. Therm. Fluid Sci.* 85 (2017), <https://doi.org/10.1016/j.expthermfluidsci.2017.03.003>.
- [56] M. Liu, Z. Zhou, Y. Chai, S. Zhang, X. Wu, S. Huang, J. Su, J. Jiang, Synthesis of Cell Composite Alginate Microfibers with the Application Potential of Small Diameter Vascular Grafts, *Biofabrication*, 2017, <https://doi.org/10.1088/1758-5090/aa71da>.
- [57] Y. Zuo, X. He, Y. Yang, D. Wei, J. Sun, M. Zhong, R. Xie, H. Fan, X. Zhang, Microfluidic-based generation of functional microfibers for biomimetic complex tissue construction, *Acta Biomater.* (2016), <https://doi.org/10.1016/j.actbio.2016.04.036>.
- [58] Y. Cheng, Y. Yu, F. Fu, J. Wang, L. Shang, Z. Gu, Y. Zhao, Controlled fabrication of bioactive microfibers for creating tissue constructs using microfluidic techniques, *ACS Appl. Mater. Interfaces* (2016), <https://doi.org/10.1021/acsami.5b11445>.
- [59] Y. Cheng, F. Zheng, J. Lu, L. Shang, Z. Xie, Y. Zhao, Y. Chen, Z. Gu, Bioinspired multicompartmental microfibers from microfluidics, *Adv. Mater.* (2014), <https://doi.org/10.1002/adma.201400798>.
- [60] T.P. Santos, A.L.R. Costa, M. Michelon, L.P. Costa, R.L. Cunha, Development of a microfluidic route for the formation of gellan-based microgels incorporating jabuticaba (*Myrciaria cauliflora*) extract, *J. Food Eng.* (2020), <https://doi.org/10.1016/j.jfoodeng.2019.109884>.
- [61] J. Atencia, D.J. Beebe, Controlled microfluidic interfaces, *Nature* (2005), <https://doi.org/10.1038/nature04163>.
- [62] C.C. Roberts, R.R. Rao, M. Loewenberg, C.F. Brooks, P. Galambos, A.M. Grillet, M.B. Nemer, Comparison of monodisperse droplet generation in flow-focusing devices with hydrophilic and hydrophobic surfaces, *Lab Chip* (2012), <https://doi.org/10.1039/c2lc21197a>.
- [63] A. Moncion, M. Lin, E.G. O'Neill, R.T. Franceschi, O.D. Kripfgans, A.J. Putnam, M.L. Fabiilli, Controlled Release of Basic Fibroblast Growth Factor for Angiogenesis Using Acoustically-Responsive Scaffolds, *Biomaterials*, 2017, <https://doi.org/10.1016/j.biomaterials.2017.06.012>.
- [64] B.M. Tiemeijer, M.W.D. Sweep, J.J.F. Sleeboom, K.J. Steps, J.F. van Sprang, P. De Almeida, R. Hammink, P.H.J. Kouwer, A.L.P.M. Smits, J. Tel, Probing single-cell macrophage polarization and heterogeneity using thermo-reversible hydrogels in droplet-based microfluidics, *Front. Bioeng. Biotechnol.* 9 (2021) 953, <https://doi.org/10.3389/fbioe.2021.715408>.
- [65] T. Mirabella, J.W.B. Macarthur, D. Cheng, C.K. Ozaki, Y.J. Woo, M.T. Yang, C.S. Chen, 3D-printed vascular networks direct therapeutic angiogenesis in ischaemia, *Nat. Biomed. Eng.* (2017), <https://doi.org/10.1038/s41551-017-0083>.
- [66] G. Gao, J.H. Lee, J. Jang, D.H. Lee, J.S. Kong, B.S. Kim, Y.J. Choi, W.B. Jang, Y.J. Hong, S.M. Kwon, D.W. Cho, Tissue engineered bio-blood-vessels constructed using a tissue-specific bioink and 3D coaxial cell printing technique: a novel therapy for ischemic disease, *Adv. Funct. Mater.* (2017), <https://doi.org/10.1002/adfm.201700798>.
- [67] C. Benwood, J. Chrenek, R.L. Kirsch, N.Z. Masri, H. Richards, K. Teetzen, S.M. Willerth, Natural biomaterials and their use as bioinks for printing tissues, *Bioengineering* 8 (2021), <https://doi.org/10.3390/bioengineering8020027>.
- [68] A.J. Melchiorri, J.P. Fisher, Bioprinting of blood vessels, in: *Essentials 3D Biofabrication Transl.*, 2015, <https://doi.org/10.1016/B978-0-12-800972-7.00020-7>.
- [69] T.D. Henry, B.H. Annex, G.R. McKendall, M.A. Azrin, J.J. Lopez, F.J. Giordano, P.K. Shah, J.T. Willerson, R.L. Benza, D.S. Berman, C.M. Gibson, A. Bajamonde, A.C. Rundle, J. Fine, E.R. McCluskey, The VIVA trial: vascular endothelial growth factor in ischemia for vascular angiogenesis, *Circulation* (2003), <https://doi.org/10.1161/01.CIR.0000061911.47710.8A>.
- [70] M. Giacca, S. Zacchigna, VEGF gene therapy: therapeutic angiogenesis in the clinic and beyond, *Gene Ther.* (2012), <https://doi.org/10.1038/gt.2012.17>.
- [71] P. Au, J. Tam, D. Fukumura, R.K. Jain, Bone marrow derived mesenchymal stem cells facilitate engineering of long-lasting functional vasculature, *Blood* (2008), <https://doi.org/10.1182/blood-2007-10-118273>.
- [72] N. Koike, D. Fukumura, O. Gralla, P. Au, J.S. Schechner, R.K. Jain, *Tissue engineering: creation of long-lasting blood vessels*, *Nature* (2004).
- [73] D.B. Kolesky, R.L. Truby, A.S. Gladman, T.A. Busbee, K.A. Homan, J.A. Lewis, 3D bioprinting of vascularized, heterogeneous cell-laden tissue constructs, *Adv. Mater.* (2014), <https://doi.org/10.1002/adma.201305506>.
- [74] J.S. Miller, K.R. Stevens, M.T. Yang, B.M. Baker, D.H.T. Nguyen, D.M. Cohen, E. Torro, A.A. Chen, P.A. Galie, X. Yu, R. Chaturvedi, S.N. Bhatia, C.S. Chen, Rapid casting of patterned vascular networks for perfusable engineered three-dimensional tissues, *Nat. Mater.* (2012), <https://doi.org/10.1038/nmat3357>.

- [75] W. Zhu, X. Qu, J. Zhu, X. Ma, S. Patel, J. Liu, P. Wang, C.S.E. Lai, M. Gou, Y. Xu, K. Zhang, S. Chen, Direct 3D Bioprinting of Prevascularized Tissue Constructs with Complex Microarchitecture, *Biomaterials*, 2017, <https://doi.org/10.1016/j.biomaterials.2017.01.042>.
- [76] I.T. Ozbolat, Y. Yu, Bioprinting toward organ fabrication: challenges and future trends, *IEEE Trans. Biomed. Eng.* (2013), <https://doi.org/10.1109/TBME.2013.2243912>.
- [77] A. Skardal, A. Atala, Biomaterials for integration with 3-D bioprinting, *Ann. Biomed. Eng.* (2015), <https://doi.org/10.1007/s10439-014-1207-1>.
- [78] V.K. Lee, A.M. Lanzi, H. Ngo, S.S. Yoo, P.A. Vincent, G. Dai, Generation of multi-scale vascular network system within 3D hydrogel using 3D bio-printing technology, *Cell. Mol. Bioeng.* (2014), <https://doi.org/10.1007/s12195-014-0340-0>.
- [79] Y.S.J. Li, J.H. Haga, S. Chien, Molecular basis of the effects of shear stress on vascular endothelial cells, *J. Biomech.* (2005), <https://doi.org/10.1016/j.jbiomech.2004.09.030>.
- [80] M. Carrabba, E. Jover, M. Fagnano, A.C. Thomas, E. Avolio, T. Richardson, B. Carter, G. Vozzi, A.W. Perriman, P. Madeddu, Fabrication of new hybrid scaffolds for in vivo perivascular application to treat limb ischemia, *Front. Cardiovasc. Med.* 7 (2020) 273, <https://doi.org/10.3389/fcvm.2020.598890>.
- [81] M. Costantini, S. Testa, E. Fornetti, C. Fuoco, C. Sanchez Riera, M. Nie, S. Bernardini, A. Rainer, J. Baldi, C. Zoccali, R. Biagini, L. Castagnoli, L. Vitiello, B. Blaauw, D. Seliktar, W. Świączkowski, P. Garstecki, S. Takeuchi, G. Cesareni, S. Cannata, C. Gargioli, Biofabricating murine and human myo-substitutes for rapid volumetric muscle loss restoration, *EMBO Mol. Med.* 13 (2021), e12778, <https://doi.org/10.15252/emmm.202012778>.
- [82] D. Xue, Y. Wang, J. Zhang, D. Mei, Y. Wang, S. Chen, Projection-based 3D printing of cell patterning scaffolds with multiscale channels, *ACS Appl. Mater. Interfaces* (2018), <https://doi.org/10.1021/acsami.8b03867>.
- [83] N. Brandenburg, M.P. Lutolf, In situ patterning of microfluidic networks in 3D cell-laden hydrogels, *Adv. Mater.* (2016), <https://doi.org/10.1002/adma.201601099>.
- [84] K.A. Heintz, M.E. Bregenzer, J.L. Mantle, K.H. Lee, J.L. West, J.H. Slater, Fabrication of 3D biomimetic microfluidic networks in hydrogels, *Adv. Healthc. Mater.* (2016), <https://doi.org/10.1002/adhm.201600351>.
- [85] C.K. Arakawa, B.A. Badeau, Y. Zheng, C.A. DeForest, Multicellular vascularized engineered tissues through user-programmable biomaterial photodegradation, *Adv. Mater.* (2017), <https://doi.org/10.1002/adma.201703156>.
- [86] R. Zhang, N.B. Larsen, Stereolithographic hydrogel printing of 3D culture chips with biofunctionalized complex 3D perfusion networks, *Lab Chip* (2017), <https://doi.org/10.1039/c7lc00926g>.
- [87] K.H. Song, C.B. Highley, A. Rouff, J.A. Burdick, Complex 3D-printed microchannels within cell-degradable hydrogels, *Adv. Funct. Mater.* (2018), <https://doi.org/10.1002/adfm.201801331>.
- [88] C. Norotte, F.S. Marga, L.E. Niklason, G. Forgacs, Scaffold-free Vascular Tissue Engineering Using Bioprinting, *Biomaterials*, 2009, <https://doi.org/10.1016/j.biomaterials.2009.06.034>.
- [89] A. Skardal, J. Zhang, G.D. Prestwich, Bioprinting Vessel-like Constructs Using Hyaluronan Hydrogels Crosslinked with Tetrahedral Polyethylene Glycol Tetracrylates, *Biomaterials*, 2010, <https://doi.org/10.1016/j.biomaterials.2010.04.045>.
- [90] C. Xu, W. Chai, Y. Huang, R.R. Markwald, Scaffold-free inkjet printing of three-dimensional zigzag cellular tubes, *Biotechnol. Bioeng.* (2012), <https://doi.org/10.1002/bit.24591>.
- [91] Y. Zhang, Y. Yu, A. Akkouch, A. Dababneh, F. Dolati, I.T. Ozbolat, In Vitro Study of Directly Bioprinted Perfusible Vasculature Conduits, *Biomater. Sci.* 2015, <https://doi.org/10.1039/c4bm00234b>.
- [92] Q. Gao, Y. He, J. zhong Fu, A. Liu, L. Ma, Coaxial Nozzle-Assisted 3D Bioprinting with Built-In Microchannels for Nutrients Delivery, *Biomaterials*, 2015, <https://doi.org/10.1016/j.biomaterials.2015.05.031>.
- [93] W. Jia, P.S. Gungor-Ozkerim, Y.S. Zhang, K. Yue, K. Zhu, W. Liu, Q. Pi, B. Yambaa, M.R. Dokmeci, S.R. Shin, A. Khademhosseini, Direct 3D Bioprinting of Perfusible Vascular Constructs Using a Blend Bioink, *Biomaterials*, 2016, <https://doi.org/10.1016/j.biomaterials.2016.07.038>.
- [94] J. Yan, Y. Huang, D.B. Chrisey, Laser-assisted printing of alginate long tubes and annular constructs, *Biofabrication* (2013), <https://doi.org/10.1088/1758-5082/5/1/015002>.
- [95] M.B. Applegate, J. Coburn, B.P. Partlow, J.E. Moreau, J.P. Mondia, B. Marelli, D.L. Kaplan, F.G. Omenetto, D.A. Weitz, Laser-based three-dimensional multiscale micropatterning of biocompatible hydrogels for customized tissue engineering scaffolds, *Proc. Natl. Acad. Sci. U. S. A* (2015), <https://doi.org/10.1073/pnas.1509405112>.
- [96] Z. Xing, C. Zhao, S. Wu, C. Zhang, H. Liu, Y. Fan, Hydrogel-based therapeutic angiogenesis: an alternative treatment strategy for critical limb ischemia, *Biomaterials* 274 (2021), <https://doi.org/10.1016/j.biomaterials.2021.120872>, 120872.